ChemComm

Structures, physicochemical properties, and applications of T–HgII–T, C–AgI–C, and other metallo-base-pairs

Journal:	*ChemComm*
Manuscript ID	CC-FEA-04-2015-002693.R1
Article Type:	Feature Article
Date Submitted by the Author:	21-Sep-2015

Complete List of Authors:	Tanaka, Yoshiyuki; Tohoku University, Laboratory of Molecular Transformation Kondo, Jiro; Sophia University, Department of Materials and Life Sciences, Faculty of Science and Technology, Sychrovský, Vladimír; Academy of Sciences of the Czech Republic, Institute of Organic Chemistry and Biochemistry Šebera, Jakub; Institute of Organic Chemistry and Biochemistry, Academy of Sciences of the Czech Republic, Molecular Spectroscopy Dairaku, Takenori; Tohoku University, Laboratory of Molecular Transformation Hisao, Saneyoshi; Kanagawa university, Department of Material and Life Chemistry, Faculty of Engineering Urata, Hidehito; Osaka University of Pharmaceutical Sciences, Torigoe, Hidetaka; Tokyo University of Science, Department of Applied Chemistry, Faculty of Science Ono, Akira; Kanagawa University, Material & Life Chemistry

Structures, physicochemical properties, and applications of T–Hg^{II}–T, C–Ag^{I}–C, and other metallo-base-pairs†

Yoshiyuki Tanaka,*[a,b] Jiro Kondo,[c] Vladimír Sychrovský,[d] Jakub Šebera,[d,e] Takenori Dairaku,[b] Hisao Saneyoshi,[f] Hidehito Urata,[g] Hidetaka Torigoe[h] and Akira Ono*[f]

[a] Faculty of Pharmaceutical Sciences, Tokushima Bunri University, 180 Nishihama-Boji, Yamashirocho, Tokushima, Tokushima 980-8578, Japan. E-mail: tanakay@ph.bunri-u.ac.jp

[b] Graduate School of Pharmaceutical Sciences, Tohoku University, 6-3 Aza-Aoba, Aramaki, Aoba-ku, Sendai, Miyagi 980-8578, Japan.

[c] Department of Materials and Life Sciences, Faculty of Science and Technology, Sophia University 7-1 Kioi-cho, Chiyoda-ku, Tokyo 102-8554, Japan

[d] Institute of Organic Chemistry and Biochemistry, Academy of Sciences of the Czech Republic, v.v.i., Flemingovo náměstí 2, 16610, Praha 6, Czech Republic

[e] Institute of Physics, Academy of Sciences of the Czech Republic, v.v.i, Na Slovance 2, CZ-182 21 Prague 8, Czech Republic

[f] Department of Material & Life Chemistry, Kanagawa University, 3-27-1 Rokkakubashi, Kanagawa-ku, Yokohama, Kanagawa 221-8686, Japan. E-mail: akiraono@kanagawa-u.ac.jp

[g] Osaka University of Pharmaceutical Sciences, 4-20-1 Nasahara, Takatsuki, Osaka 569-1094, Japan

[h] Department of Applied Chemistry, Faculty of Science, Tokyo University of Science, 1-3 Kagurazaka, Shinjuku-ku, Tokyo 162-8601, Japan

Abstract

Recently, metal-mediated base-pairs (metallo-base-pairs) have been studied extensively with the aim of exploring novel base-pairs; their structures, physicochemical properties, and applications have been studied. This trend has become more evident after the discovery of Hg^{II}-mediated thymine–thymine (T–Hg^{II}–T) and Ag^{I}-mediated cytosine–cytosine (C–Ag^{I}–C) base-pairs. In this article, we focus on the basic science and applications of these metallo-base-pairs, which are composed of natural bases.

Introduction

Studies on metal-mediated base-pairs (metallo-base-pairs) were initiated in the light of material sciences and genetic code expansion.[1,2] K. Tanaka and Shionoya proposed the possibility that Watson–Crick (W–C) base-pairs may be substituted for planar metal chelators.[1] Meggers, Romesberg, and Schultz actually introduced such a metal chelator into DNA duplexes, and they proposed that such a metallo-base-pair would lead to the expansion of the genetic code.[2] K. Tanaka and Shionoya also introduced their metal chelator into a DNA duplex to generate a molecular magnet,[3] and they showed that the aligned paramagnetic Cu^{2+} ions in the DNA duplex were ferromagnetically coupled.[4] Since then, many metallo-base-pairs have been created through the use of artificial metal chelators, and DNA duplexes including such metallo-base-pairs (metallo-DNAs) have been reported (for their structures and the corresponding references, see Figure S1 in the ESI†).

As an alternative approach to the creation of novel metallo-base-pairs, it is interesting to examine if natural nucleobases can form metallo-base-pairs. In fact, thymine can specifically bind to Hg^{2+} to form an Hg^{II}-mediated T–T base-pair (T–Hg^{II}–T, Figure 1).[5,6] In addition, this Hg^{2+}-specific recognition by thymine has been applied to an Hg^{2+} sensor.[5] Later, it was found that cytosine also binds to Ag^{+} to form an Ag^{I}-mediated C–C base-pair (C–Ag^{I}–C, Figure 1), and an Ag^{+} sensor was developed based on this phenomenon.[7] Since such natural-nucleobase-based Hg^{2+} and Ag^{+} sensors can be prepared from commercially available sources, and because Hg^{2+} is an environmental pollutant, scientists from different fields have joined the studies on the metallo-base-pairs to applied them as metal sensors, single-nucleotide-polymorphism (SNP) detectors, heavy-metal trappers, nanomachines, etc.[8-15]

Although many applications of the metallo-base-pairs have been reported (see the review articles[8-15] and the references cited therein), the basic science of these metallo-base-pairs is also as versatile as their applications, because the resulting structural, thermodynamic, and other fundamental physicochemical data and parameters are universally applicable to the design and creation of molecular devices. In this sense, we would like to review studies on metallo-base-pairs, those composed of natural bases and related unnatural bases whose physicochemical studies were performed. Our review is divided into the following sections: spectroscopy (section 1.1), crystallography (section 1.2), thermodynamics (section 1.3), theoretical studies (section 1.4),

applications as metal sensors (section 2.1), Hg^{2+} trapping (section 2.2), SNP detection (section 2.3), nanomachines (section 2.4), conductivity (section 2.5), and response to enzymes (section 2.6).

1.1) Metallo-base-pairs in solution: spectroscopic studies

One of the advantages of metallo-base-pairs is that programmed metal-ion arrays can be prepared in DNA duplexes in solution. Thus, properties and structures of metallo-base-pairs in solution are of prime interest. Based on these concepts, chemical structures of metallo-base-pairs as well as 3D structures of two DNA duplexes containing metallo-base-pairs were determined with NMR spectroscopy in solution.[16-22] One is a Ag^{I}-mediated imidazole–imidazole base-pair (Im–Ag^{I}–Im), which employs an artificial nucleobase (imidazole),[19,21] and the other is an Hg^{II}-mediated T–T base-pair (T–Hg^{II}–T), which employs a natural nucleobase (thymine).[16,17,20,22] In both cases, the chemical structures of these metallo-base-pairs were solidly determined on the basis of N-N and N-Ag *J*-coupling (Figure 2; details are discussed later).[16,19] Furthermore, 3D structures of DNA duplexes containing these metallo-base-pairs were determined with NMR spectroscopy (Figure 2).[19,21,22] In the case of the T–Hg^{II}–T base-pair, its crystal structure in a DNA duplex was also determined (see next section for details).[23] Therefore, the T–Hg^{II}–T base-pair currently is the best benchmark for studying the relationship between the structure and spectroscopic data in solution.

In addition to the abovementioned structural studies, there are many spectroscopic studies of metallo-base-pairs. Especially, the T-Hg^{II}-T base-pair possesses the longest history of all metallo-base-pairs, and it has been extensively studied by Raman,[20,24,25] IR,[25] UV,[6,26,27] circular dichroism (CD)[6,26,28,29] and NMR[6,16,17,27,30,31] spectroscopic techniques from its proposal based on the studies at its early stage (~50 years ago)[32]. In addition, Hg^{2+}-titration studies of poly[d(AT)] using ^{1}H NMR spectroscopy might be related to T–Hg^{II}–T base-pairing.[33] The U–Hg^{II}–U base-pair (Figure 3a), the RNA analogue of the T–Hg^{II}–T base-pair, was also studied by ^{1}H NMR spectroscopy.[34]

Other metallo-base-pairs (A–Hg^{II}–T and C–Ag^{I}–C) in DNA duplexes were studied with NMR spectroscopy. Extensive ^{15}N chemical-shift analyses revealed the chemical structure of the A–Hg^{II}–T base-pair (Figure 3b) in a DNA duplex (the ^{15}N chemical shifts are discussed later).[35-38] For the C–Ag^{I}–C base-pair, a Ag^{I}-titration study of a single-C–C-mismatch-embedded DNA duplex was performed with ^{1}H NMR spectroscopy.[7] Stacking of the C–Ag^{I}–C base-pair within a DNA duplex was strongly suggested by a slow-exchange phenomenon observed in the ^{1}H NMR spectra, in which NMR signals from Ag^{I}-bound and Ag^{I}-free states were observed independently.[7] However, the exact base-pairing mode of C–Ag^{I}–C has not yet been determined. The U–Ag^{I}–U base-pair (2:3 complex between 1-methyluracyl and Ag^{+}) was also studied with IR and Raman spectroscopy, by using its crystalline sample (Figure 3c).[39] See reference 18 and references cited therein for other simple Hg^{II}–DNA/nucleoside/nucleotide complexes.

In addition, possible metallo-base-pairs in a kind of metallated DNA molecules, so-called M-DNA[40-42] were studied. In M-DNA, penetration of Zn^{2+} into W–C base-pairs to afford metal-mediated base-pairs was suggested by fluorescence and ^{1}H NMR spectroscopy.[40-42] However,

the base-pairing pattern has not yet been determined, and several possible models are presented.[40,43,44]

Based on the similarity between the transoid C–Ag^{I}–C base-pair[45-48] (Figure 1c) and the hemiprotonated transoid C–C base-pair in i-motif, an i-motif-type structure composed of transoid C–Ag^{I}–C base-pairs was proposed on the basis of CD and fluorescence spectroscopy.[46]

In the case of a hydroxypyridone–Cu^{II}–hydroxypyridone base-pair (H–Cu^{II}–H) (Figure 3d), an average Cu^{II}–Cu^{II} distance of ~3.7 Å was determined with EPR spectroscopy for a DNA duplex containing five H–Cu^{II}–H base-pairs.[4] The Cu^{2+} ions in the H–Cu^{II}–H base-pairs were ferromagnetically coupled[4] and structural reasons for the ferromagnetic coupling were theoretically studied.[49]

As an overview of this section, characteristic NMR and vibrational spectroscopic features of the metallo-base-pairs are summarised in Tables 1–3. The ^{13}C NMR spectrum of the T–Hg^{II}–T base-pair revealed that the carbonyl-carbon resonances for C4 and C2 were shifted downfield by ~2.5 ppm upon Hg^{II}-complexation in dimethyl sulfoxide (DMSO) and H_2O (Table 1).[20,30] More drastic changes in chemical shifts were observed for the ^{15}N resonances of the metal-binding nitrogen atoms, namely, ca. +30 ppm (downfield shift) for N3 of the T–Hg^{II}–T base-pair (N3(T))[16,17] and ca. -15 ppm (upfield shift) for N3 of the Im–Ag^{I}–Im base-pair (N3(Im))[19] (Table 2). For the A–Hg^{II}–T base-pair, the Hg^{II}-ligated site was deduced to be N6 (the amino nitrogen) and not N1. This deduction is based on careful considerations of the changes in chemical shifts of the N1 atom of the adenosine residue (N1(A)) upon Hg^{2+}-binding, despite the fact that a large change in chemical shift of N1(A) occurs (+9.4 to +15.3 ppm) (Table 2).[35-38] As a general rule,[17] the formation of an N–metal coordination bond causes an upfield shift of the ^{15}N resonance (as observed for the Im–Ag^{I}–Im base-pair and similar systems)[50-54], whereas proton–metal exchange on a nitrogen atom causes a downfield shift (as observed for the T–Hg^{II}–T base-pair)[16-18]. Applying these general trends to the A–Hg^{II}–T base-pair, coordination of N1(A) to Hg^{II} was ruled out, because a downfield shift of N1(A) was observed. Further details and backgrounds regarding heteronuclear NMR chemical shifts are reviewed in references 17 and 18.

Two-bond ^{15}N-^{15}N *J*-coupling across Hg^{II}, $^{2}J(^{15}N,^{15}N)$, was observed for the T–Hg^{II}–T base-pair of the DNA duplex with the paired thymine bases ^{15}N-labeled (Table 2).[16,17] The observation of $^{2}J(^{15}N,^{15}N)$ firmly demonstrates the formation of a ^{15}N3(T)–Hg^{II}–^{15}N3(T) linkage in the T–Hg^{II}–T base-pair. At the same time, the large downfield shift of N3(T) indicates the low covalency (highly ionic nature) of the N3(T)–Hg^{II} bond (high percentage of ionicity and low percentage of covalency).[17] In addition, 1-bond ^{199}Hg-^{15}N *J*-coupling, $^{1}J(^{199}Hg,^{15}N)$ = 1050 Hz,[18] was recently reported for the thymidine–Hg^{II}–thymidine complex with its ^{199}Hg NMR chemical shift, $\delta(^{199}Hg)$ = -1784 ppm[18,30c]. For the Im–Ag^{I}–Im base-pair, 1-bond *J*-coupling between ^{15}N and $^{107}Ag/^{109}Ag$ at natural abundance ($^{1}J(^{15}N,^{107/109}Ag)$) was observed (Table 2).[19] The observation of $^{1}J(^{15}N,^{107/109}Ag)$ confirms the formation of N3(Im)–Ag^{I} linkages in the Im–Ag^{I}–Im base-pair. In a chemical sense, such spectroscopic data, especially *J*-coupling and chemical shifts of heteronuclei

in NMR spectroscopy, provide essential information for the characterisation of metal–nitrogen bonds.

Raman spectroscopic studies were performed on the T–Hg^{II}–T and U–Ag^{I}–U base-pairs.[20,25,39] Several marker bands for both base-pairs are listed in Table 3. An extraordinarily low-wavenumber-shifted C4=O4 stretching band was observed at 1586/1585 cm^{-1} for the T–Hg^{II}–T base-pair.[25,20] This extraordinary band was firmly assigned on the basis of an isotope shift of the Raman band by ^{18}O-labeling at the O4 atom. A similar shift to low wavenumber was observed for the C4=O4 stretching band of the U–Ag^{I}–U base-pair (Table 3).[39] We then identified that a Raman band at 749 cm^{-1} is the marker band to probe the existence of imino proton (H3) of thymine (Table 3).[20] Disappearance of this band indicates the deprotonation of H3 (imino proton) of thymine (Table 3).[20] The Raman/IR bands described above can be used as marker bands to detect T–Hg^{II}–T and U–Ag^{I}–U base-pairs.

An ionic nature (low covalency) of the N3(T)-Hg^{II} bond was deduced again for the T–Hg^{II}–T base-pair from the low-wavenumber-shifted C4=O4 stretching band at 1586/1585 cm^{-1}, by consideration of an enolate-like resonance contributor (Figure 4).[20,25] Both the NMR[17] and vibrational spectroscopic[20] data thus corroborate the significantly ionic character of the N3(T)–Hg^{II} bond and the cationic nature of Hg^{II}; this was also confirmed theoretically[20] (see section 1.4 for theoretical studies). Usually, spectroscopic parameters acquired from macromolecules, such as DNA oligomers, are not so precisely determined because of low sensitivities/resolutions. However, owing to the site-specific ^{15}N- and ^{18}O-labelling of critical atoms and proper choices of measurement conditions, the spectroscopic data described above have been precisely determined to reveal physicochemical properties and even electronic structures of metallo-base-pairs.

Furthermore, the derived electronic structure suggested the application of the T–Hg^{II}–T base-pair in conductive nanowires. The cationic nature of Hg^{II} in the T–Hg^{II}–T base-pair suggests that the Hg^{II} array may function as an electron acceptor,[17b] and the Hg^{II} array in a tract of T–Hg^{II}–T base-pairs could provide a route for excess electrons.

In summary, NMR spectroscopy and (partly) Raman spectroscopy provide accurate information about the chemical structures of metallo-base-pairs, since these techniques can provide information on their local geometries around metal centres from NMR signals of the metal cation-binding atoms (or from Raman bands that arise from vibrations around the metal cations). Based on these chemical structures, the 3D structures of metallo-DNAs containing metallo-base-pairs were precisely determined. In addition, the spectroscopic data include plenty of information about the electronic structures of metallo-base-pairs, which will provide guidelines for the creation of nanoelectronic devices.

1.2) Metallo-base-pairs in crystal: crystallographic studies

X-ray crystallography is one of the best methods for obtaining accurate 3D structures of metallo-base-pairs and of metallo-DNAs that contain them. In 2001, Schultz and coworkers reported the first crystal structure of a nucleic acid duplex containing a metallo-base-pair.[55] In their

previous work,[2] they found that a 15-nucleotide DNA duplex containing the artificial Cu^{II}-mediated base-pairs with pyridine-2,6-dicarboxylate (Dipic) and pyridine (Py) (Dipic–Cu^{II}–Py) in the middle displayed thermal stability comparable to that of a duplex containing an A–T base-pair instead. A DNA fragment with the sequence d(CGCG(Dipic)AT(Py)CGCG) was crystallised in the presence of 1 equivalent of Cu^{2+}, and the crystal structure was determined at a resolution of 1.5 Å. The DNA fragment was crystallised as a Z-form left-handed duplex (Figure 5a). In the helix, Dipic forms a Cu^{II}-mediated base-pair with Py (Figure 5b). In the base-pair, Dipic and Py had anti and syn conformations about the glycosyl bonds, respectively. The Cu^{2+} ion was located between the Dipic and Py bases and had a square-planar coordination geometry. The distances from Cu^{II} to N3(Dipic) and N3(Py) are both 1.9 Å and the N3(Dipic)–Cu^{II}–N3(Py) bond was linear. Cu^{II} was also ligated with O2a(Dipic) and O4a(Dipic), with distances of 2.2 and 2.2−2.3 Å, respectively. In addition to the square-planar coordination, Cu^{II} underwent electrostatic interaction from the axial direction of the square-planar geometry by the deoxyribose O4′ atom of the neighbouring T7 residue. The distance from Cu to O4′ is 3.0−3.2 Å (Figure 5c). Axial interaction is possible only in the Z-form conformation. On the opposite side, Cu^{II} was in close proximity (3.1−3.2 Å) to the electron-rich O6(G) atom of the neighbouring residue (Figure 5c), suggesting the existence of an electrostatic interaction between them. Although the C1′−C1′ distance is 9.2−9.4 Å (Figure 5b), which is 1.3−1.5 Å shorter than those observed in canonical W−C base-pairs (ca. 10.7 Å), the overall Z-form conformation was not distorted.

In 2011, another crystal structure of a DNA duplex containing an artificial metallo-base-pair, determined at a resolution of 2.2 Å, was reported by Carell and coworkers.[56] Two DNA fragments containing salicylic aldehyde (S) were cocrystallised with a DNA polymerase of *Thermococcus kodakaraensis* (KOD XL DNA polymerase) in the presence of Cu^{2+} ions. In the protein−DNA complex, the DNA took a right-handed duplex containing a Cu^{II}-mediated S−S base-pair (S−Cu^{II}−S) at the centre (Figure 6a). The S base cannot form a pair with itself in the absence of Cu^{2+}. However, in the presence of Cu^{2+} and ethylenediamine, the S bases form the S−Cu^{II}–S base-pair (Figure 6b), just like the authors had designed in their initial concept[10,57]. The two S bases are reversibly cross-linked by an ethylenediamine bridge, which forms a bisimine system. As observed for the Dipic−Cu^{II}–Py base-pair discussed earlier, Cu^{II} is located between the two S bases and had a square-planar coordination geometry, being ligated with two O3 and two N4 atoms of the S bases. The distances from Cu^{II} to O3 and N4 are 1.8−2.0 and 2.0−2.3 Å, respectively (Figure 6b). In vertical directions, Cu^{II} underwent electrostatic interactions with the N1(A) and N1(G) atoms of neighbouring residues, with distances of 3.6 and 3.7 Å, respectively (Figure 6c). The C1′–C1′ distance (11.4 Å) is slightly longer than those of canonical W–C base-pairs (Figure 6b). It is noteworthy that various DNA polymerases incorporate deoxyribosyl salicylic aldehyde with 5'-triphosphate (dSTP) against S residues of the template DNA strand in the presence of Cu^{2+} and ethylenediamine.

An artificial metallo-base-pair was also observed in a crystal structure of a GNA (glycol nucleic acid) duplex determined at a resolution of 1.3 Å by Meggers and coworkers in 2008.[58] Since

GNA has the structurally most simple phosphodiester-containing nucleic acid backbone, GNA is considered to be a promising candidate for an initial genetic molecule of life.[59] The self-complementary (*S*)-GNA fragment g(CGHATHCG), containing two artificial hydroxypyridone (H) bases, forms a right-handed duplex that is significantly different from the B- and A-form nucleic acid helices (Figure 7a). In the GNA duplex, Cu^{2+} ions specifically bound to two H−H mismatches, so that two H−Cu^{II}−H base-pairs are formed. Again, Cu^{II} is located between the two bases and is coordinated, in a square-planar fashion, by four oxygen atoms (Figure 7b). The distances from Cu^{II} to the O3 and O4 atoms of the H nucleobases are 1.9−2.0 Å (Figure 7b). Four electrostatic interactions are also observed in vertical directions: from Cu^{II} to N1(C), O2(C), N7(A), and N9(A), with distances of 3.3, 3.8, 3.6, and 3.4 Å, respectively (Figure 7c). The C1′−C1′ distance in the H−Cu^{II}−H base-pair (12.7 Å) is 2.0 Å longer than those of standard W−C base-pairs (Figure 7b), but the Cu^{II}-mediated base-pairs fit well into the overall GNA duplex structure without any severe distortions.

The first metallo-base-pair composed of natural nucleobases was observed in a crystal structure of the duplex form of the HIV-1 RNA dimerisation-initiation site, and was reported by Dumas and coworkers in 2003.[60] In their comprehensive studies of interactions between metal ions and RNA duplexes, unexpected binding of an Au^{3+} ion with a G−C base-pair was observed in a crystal structure determined at a resolution of 2.3 Å (Figure 8a). The Au^{3+} ion induced deprotonation at N1(G) and bound between the W−C edges of G and C to form a Au^{III}-mediated G−C base-pair (G−Au^{III}−C). The distances from Au^{III} to N1(G), N2(G), O2(C), and N3(C) are 1.6−1.7, 2.3−2.4, 2.6, and 2.3−2.4 Å, respectively (Figure 8b). Due to the close proximity of Au^{III} and N2(G), Dumas and coworkers suggested that the two hydrogen atoms of the N2 amino group might be pushed away perpendicularly to the plane of the base-pair. The Au^{3+} ion is in close contact with electron-rich N7(G), N1(A), and N6(A) in vertical directions, with distances of 3.4, 3.6−3.8, and 3.6−3.7 Å, respectively (Figure 8c). The C1′−C1′ distance in the G−C base-pair is enlarged to 10.9−11.1 Å by the Au^{3+}-binding (Figure 8b), but the G−Au^{III}−C base-pair does not distort the A-form RNA duplex. The G−Au^{III}−C base-pair has not been observed in solution so far, and it is unclear whether this metallo-base-pair can stably exists in solution. If it exists, there remain unresolved issues, such as the hybridisation state of N2 (N2 pyramidalisation) and the possibility of an amino-proton−Au^{3+} exchange at N2(G).

Recently, we determined the crystal structure of a B-form DNA duplex containing two contiguous T−Hg^{II}−T base-pairs (metallo-DNA(T−Hg^{II}−T)) at a resolution of 2.7 Å.[23] A pseudo-self-complementary DNA fragment containing two contiguous T−T mismatches took the B-form conformation upon specific binding of Hg^{2+} to the T−T mismatches, thereby forming two contiguous T−Hg^{II}−T base-pairs (Figure 9a). In the T−Hg^{II}−T base-pair, the Hg^{II} was located between two T bases (Figure 9b). The distance between N3(T) and Hg^{II} was 2.0 Å, which indicates that the N3 atom has lost an imino proton even at neutral pH (the DNA duplex was crystallised at pH 7.0, and the pK_a value at the N3(T) is 9.8), which agrees with previous NMR measurements in solution[6,16,27] (section 1.1). The local geometries of the metal linkages in the T−Hg^{II}−T base-pairs

were basically identical to that observed in the crystal structure of a 2:1 complex between 1-methylthymine and Hg^{II}.[61] The propeller-twist angles of the T−Hg^{II}−T base-pairs (-22° and -20°) were remarkably larger than those of canonical W−C base-pairs in the B-form DNA duplex (-1°). This is probably because of no extra bond except for the N3-Hg^{II}-N3 linkage in the T−Hg^{II}−T base-pairs and because of repulsion between carbonyl groups O2 and O4. The C1′−C1′ distance was 9.5−9.6 Å (Figure 9b), which is about 1 Å shorter than those of canonical W−C base-pairs. However, the B-form conformation was not distorted. The distance between the two Hg^{II} was 3.3 Å. The relatively short distance between the two Hg^{2+} cations indicates that a metallophilic attraction between Hg^{II} may exist (Figure 9c) (see section 1.4 for metallophilic attraction). Hg^{II} of the tandem T−Hg^{II}−T base-pairs underwent electrostatic interactions with N1(A) and N6(A) atoms of neighbouring A−T base-pairs, with distances of 3.6−3.7 and 3.7−3.9 Å, respectively (Figure 9c). In the absence of Hg^{2+}, the middle DNA segment that contains T-T mismatches takes an unusual nonhelical conformation containing two contiguous A−T−T triplets. This suggests that the Hg^{2+} ions are necessary for stabilising the B-form conformation, at least in this sequence context. Crystal structures of other types of nucleoside/nucleotide−Hg^{II} complexes are discussed in the review by Y. Tanaka and Ono.[17b]

The crystallographic structures of metallo-base-pairs and metallo-DNAs provide accurate 3D coordinates of the atoms. Even if the crystal lattice sometimes modulates or alters the molecular structures due to crystal-packing, the crystallographically derived 3D structures can be used as a reliable structural template for designing molecular devices.

1.3) Thermodynamics of metallo-base-pairs

Thermodynamic parameters (ΔG, ΔH, ΔS, and K_d) are useful fundamental physicochemical data. Once they have been determined for a metallo-base-pair of interest, one can theoretically estimate how much metallo-DNA with the designated metallo-base-pair is formed under given physical and chemical conditions. In addition, thermal denaturation experiments using UV absorbance, and the resulting T_m values, have been used for the detection of the formation of metallo-base-pairs.

Thermal denaturation experiments using UV absorbance showed that the addition of Hg^{2+} [6,62] and Ag^{+} [7,63] significantly stabilised DNA duplexes that contain T–T and C–C mismatches, respectively. However, DNA duplexes in which T–T or C–C mismatches were substituted for other base-pairs/mismatches were not significantly stabilised by the addition of Hg^{2+} [62] and Ag^{+}[63]. With regard to metal-cation specificities of T–T and C–C mismatches, metal ions other than Hg^{2+} and Ag^{+} (such as Mg^{2+}, Ca^{2+}, Mn^{2+}, Fe^{2+}, Fe^{3+}, Co^{2+}, Ni^{2+}, Cu^{2+}, Zn^{2+}, Ru^{3+}, Pd^{2+}, Cd^{2+}, and Pb^{2+}) did not stabilise either DNA duplexes with a T–T mismatch[6] or a C–C mismatch[7]. Thus, the combinations of Hg^{2+} with the T–T mismatch and Ag^{+} with the C–C mismatch are highly specific.

Isothermal titration calorimetric (ITC) analyses revealed that the molar ratios between Hg^{2+} and the T–T mismatch[62] and that between Ag^{+} and the C–C mismatch[63] were both 1:1 (Table 4). Both binding constants are nearly 10^6 M^{-1} (Table 4),[62,63] which is significantly larger than those observed for nonspecific metal-ion–DNA interactions. Negative enthalpy changes and positive entropy

changes were observed for binding of the metal ions (Table 4).[62,63] The observed positive entropy changes may mainly result from the positive dehydration entropy due to the release of structured water molecules surrounding Hg^{2+} and Ag^{+} upon binding to the mismatches. In fact, complete shielding of Hg^{II} from solvent water molecules was observed in 3D structures of DNA duplexes containing T–Hg^{II}–T base-pairs (Figures 2a and 9c).[22,23] The observed negative enthalpy change may be mainly driven by the negative binding enthalpy due to the formation of N3–Hg^{II}–N3 and N3–Ag^{I}–N3 linkages. These conclusions on the T–Hg^{II}–T base-pair were later supported by theoretical calculations of thermodynamic parameters (Table 4), based on a possible reaction scheme proposed for the specific binding of Hg^{2+} to the T–T mismatch.[22,64] Similar thermodynamic properties were obtained from ITC analyses of the formation of artificial Im–Ag^{I}–Im base-pairs, i.e., positive entropy and negative enthalpy changes (Table 4).[65]

ITC analyses of the Hg^{2+}-binding to the two neighbouring T–T mismatches in a DNA duplex revealed a significantly larger affinity for the binding of the second Hg^{2+} than for the first Hg^{2+} (Table 5).[66] Positively cooperative binding may be favourable for the alignment of multiple Hg^{II} in a DNA duplex for the application of metallo-base-pairs in nanotechnology. Positively cooperative binding was also deduced from ITC analyses of the binding between Ag^{+} and a DNA duplex containing two neighbouring Im–Im mismatches (Table 5).[65] By contrast, the cooperative effect was not observed for the binding of Ag^{+} to two neighbouring C–C mismatches (Table 5).[67] The observed cooperativity of Hg^{II} in T–Hg^{II}–T base-pairs and Ag^{I} in Im–Ag^{I}–Im base-pairs may be explained by the attraction between heavy metals (metallophilic attraction)[68,69] (see next section for the metallophilic attraction). In relation to the T–Hg^{II}–T base-pair, thermal denaturation experiments of complexations of Hg^{2+}/Ag^{+} with 5-substituted uracil/thymine and 2-thiothymine/4-thiothymine within DNA duplexes are reported in references-70 and 71.

1.4) Theoretical studies of metallo-base-pairs

Electronic structures of metallo-base-pairs, as deduced from theoretical calculations, can often provide hints on how to tune the properties of metallo-DNAs for use in specific molecular nanodevices. To obtain realistic electronic structures of metallo-base-pairs in nanodevices, reliable 3D structures (models) under working conditions of these nanodevices are required. However, current structural data do not include all of the possibilities, such as sequence/conformational varieties of metallo-DNAs and variations in physical conditions. To overcome this issue, structural interpretation of NMR and optical spectroscopic parameters, employing theoretical methods, has been recognised as a valuable method for the elucidation of 3D structures of not only metallo-base-pairs and metallo-DNAs, but also of any molecule of interest under the given conditions. Therefore, we review theoretical calculations of spectroscopic parameters of T–Hg^{II}–T and related base-pairs. In addition, the metallophilic attraction is discussed as a recent topic in the fields of inorganic chemistry and metallo-DNA.

The formation of the T–Hg^{II}–T base-pair was first demonstrated from the observation of $^{2}J(^{15}N,^{15}N)$ across the metal linkage.[16] The the zeroth-order regular approximation density

functional theory (ZORA DFT) calculations of $^{2}J(^{15}N,^{15}N)$ later confirmed the existence of the N–Hg^{II}–N linkage in the T–Hg^{II}–T base-pair, and showed agreement between the experimental and calculated $^{2}J(^{15}N,^{15}N)$ values.[72] DFT calculations of Raman spectra of T–Hg^{II}–T base-pair confirmed the assignment of the C4=O4 stretching vibration of the T–Hg^{II}–T base pair (Table 3) and unveiled the significant cationic character of the Hg^{II} in the T–Hg^{II}–T basepair.[20,73] Time-dependent-DFT (TD-DFT) calculations of UV absorption spectra of DNA duplexes containing T–Hg^{II}–T base-pairs elucidated the character of the stacking interaction between consecutive T–Hg^{II}–T base-pairs.[74]

Structural and electronic-structural studies of other metallo-base-pairs were also performed. DFT calculations corroborated the structural studies of Hg^{II}- and Ag^{I}-mediated base-pairs with azole nucleosides.[75] The structure, chemical bonding, and formation of a Ag^{I}-mediated Hoogsteen-type thymine-1,3-dideazaadenine base-pair was studied using the ZORA DFT-D method.[76] Cu^{+}/Ag^{+}/Au^{+}-mediated base-pairs composed of natural nucleobases and 1-deazaadenine were studied using the B3LYP-D3 DFT method.[77] The binding of several metal cations to H (hydroxypyridone) and derived nucleobases, as well as the resulting metallo-base-pairs, were calculated using DFT methods.[78] The DFT calculations further suggested an Ag^{I}-mediated uracil–uracil base-pair[79] which took a slightly different structure from the metallo-base-pair of the 2:3 complex between 1-methyluracil and Ag^{+} [39] (Figure 3c).

There are several studies on the attraction between heavy metals (metallophilic attraction) in metallo-base-pairs and metallo-DNAs. Heavy-metal cations in metallo-DNAs may exhibit unexpected properties. It was reported that Hg^{2+}, Ag^{+}, and several other heavy-metal cations in organometallic compounds do not repel each other, despite their cationic nature, because of the metallophilic attraction between these metals.[68,69] Stabilisation owing to metallophilicity is assumed to occur for metal–metal contacts ranging from ca. 3.2 to 4.0 Å, based on relatively short metal–metal distances in crystals. Metallophilic attraction may therefore be operative in metallo-DNAs, because the separations between consecutive base-pairs in normal nucleic acids fall in this range. Møller-Plesset theory (MP2) and spin-component-scaled MP2 (SCS-MP2) calculations of two U–Hg^{II}–U base-pairs unveiled significant stabilisation owing to metallophilicity.[80] In particular, the Hg^{II}–Hg^{II} interaction in tandem U–Hg^{II}–U base-pairs contributes 9% to the total stabilisation, despite the significant cationic character of the Hg^{II} in U–Hg^{II}–U base-pairs.[80] The stabilising role of the metallophilic attraction is also seen in the 3D structure of metallo-DNA containing tandem T–Hg^{II}–T base-pairs, showing short Hg–Hg distances in the B-form duplex.[22,23] Stabilisation owing to metal–metal interactions was also calculated for Ag^{I}–Ag^{I} contacts in the thymine-1,3-dideazaadenine base-pair[76] and for the Im–Ag^{I}–Im base-pair.[21] Although direct experimental evidence for the metallophilic attraction is still missing, the experimentally observed contacts (~3.3 Å) between Hg^{II} in metallo-DNA(T–Hg^{II}–T) suggested that its existence is plausible.[23] Theoretical interpretation of UV absorption spectra of two contiguous T–Hg^{II}–T base-pairs unveiled spectral characteristics that are partly induced by metal–metal interactions.[74] A one-bond ^{109}Ag-^{109}Ag *J*-coupling constant ($^{1}J(^{109}Ag,^{109}Ag)$) of ~1 Hz was

calculated for consecutive Im–Ag^{I}–Im base-pairs using the ZORA DFT method; thus, measurement of $^{1}J(^{109}Ag,^{109}Ag)$ provides a possible way to detect the metallophilic attraction, but the value would be too small for practical detection.[81]

The rational design and optimisation of metallo-DNAs for their use in technological applications could be achieved through knowledge of their 3D structures and properties, as deduced from thermodynamic and spectroscopic parameters (see sections 1.1 and 1.2 for currently available 3D structures of metallo-DNAs).[49,82-85] Knowledge of the 3D structure of metallo-DNA containing Im–Ag^{I}–Im base-pairs allowed for reliable TD-DFT calculations of electronic and optical properties.[85] The thorough structural characterisation of the T–Hg^{II}–T base-pair, employing spectroscopic data in conjunction with the 3D structure of metallo-DNA(T–Hg^{II}–T), allowed us to calculate thermodynamic parameters for the T–Hg^{II}–T base-pairing by using the ONIOM (B3LYP:BP86) method (Table 4).[64] The calculated thermodynamic parameters were consistent with the experimental parameters (Table 4).[62]

The use of metallo-DNAs as nanowires in the field of nanoelectronics is one of several promising applications (see section 2.5 for charge-transport experiments and conductivity measurements). The array of metals embedded in the metallo-DNA scaffold could possess desirable charge-transport properties. DFT calculations of tandem T–Hg^{II}–T base-pairs suggested that the frontier orbitals may enhance the transport of excess electrons rather than holes.[86] The enhanced conductivity of DNA base-pairs owing to their modification with copper was calculated using the DFT method with Green's function technique.[87] Theoretical calculations of the electron conductivity of artificial metallo-base-pairs further showed that the electron transport might be controlled by an external magnetic field.[88] Theoretical DFT calculations indicated that the hole-transport efficiency in a DNA molecule containing a T–Hg^{II}–T base-pair or a T–T mismatch is affected particularly by the spatial overlap between neighbouring base-pairs; this overlap is higher for the Hg^{II}-mediated base-pair.[89]

To summarise, theoretical calculations of metallo-DNA(T–Hg^{II}–T) provided its precise structure, which is consistent with experimental NMR spectroscopic and thermodynamic parameters. The structure and the results of the calculation provided further information on the electronic structures of metallo-DNA(T–Hg^{II}–T)s, whose structures were both spectroscopically and theoretically proven. Thus, based on the agreement between calculations and experiments, theoretical calculations provided and will continue to provide realistic physicochemical properties of metallo-DNAs. The estimated physicochemical properties will be further used for the optimisation of the properties of metallo-DNAs for their use in technologies such as conductive nanowires.

2.1) Application in metal sensors

The most successful applications of T–Hg^{II}–T and C–Ag^{I}–C base-pairs are in metal sensors, which are chemical probes for the detection of Hg^{2+} and Ag^{+} ions in aqueous solutions.[5,7] In 2004, Ono and Togashi reported a fluorescence resonance energy transfer (FRET)-based Hg^{2+} sensor in which

the fluorescence is quenched upon the formation of T–Hg^{II}–T base-pairs.[5] Since then, oligonucleotide-based Hg^{2+} sensors using various mechanisms of detection have been developed. A similar Ag^{+} sensor based on the C–Ag^{I}–C base-pairing ability of cytosine has also been developed.[7] For more details on metal sensors, refer to reviews that have been published in recent years;[11,13,90-94] metal sensors reviewed in those references are summarised in Figure 10.

2.2) Application in Hg^{2+} trapping

The specific recognition of Hg^{2+} by thymine was applied to Hg^{2+}-trapping agents. The Hg^{2+}-trapping agents can be classified into two types: thymine/uracil-monomer-based Hg^{2+}-trapping agents and DNA-oligomer-based agents (Figure 11). The monomer-based ones include thymine-cross-linked polystyrene beads[95] and uracil-cross-linked polystyrene fibres,[96] and DNA-oligomer-based ones include thymidine-rich-DNA-cross-linked polyacrylamide,[97] T-rich-DNA-cross-linked microparticles,[98] oligo-T-cross-linked polystyrene beads,[99,100] and T-rich-DNA-cross-linked silica gel.[101]

The thymine/uracil-cross-linked polymer has a high density of Hg^{2+}-binding ligands (thymine/uracil) on its polymer surface,[95,96] although the affinity against Hg^{2+} for each binding site is not so high. On the other hand, the ligand densities do not need to be high for the T-rich-DNA-cross-linked solid support, but the affinity against Hg^{2+} for each binding site is high. Most Hg^{2+}-trapping agents can selectively capture Hg^{2+} in the presence of other cations.[95-98,100,101] More interestingly, the Hg^{2+}-trapping efficiency of T-rich-DNA-cross-linked polystyrene beads was higher in the presence of other cations, which is favourable for their use under natural conditions.[100] In addition, the Hg^{2+}-trapping agents could be recycled several times.[95-98,101]

2.3) Detection of single-nucleotide polymorphisms (SNPs)

The specific binding of Hg^{2+} to a T–T mismatch was used for the detection of single-nucleotide polymorphisms (SNPs).[102] For SNP detection, an SNP probe DNA oligomer containing a 19-mer loop sequence, flanked by thymidine heptamers (T_7) at the 5′ and 3′ sides of the loop, was prepared (Figure 12). This SNP probe DNA oligomer was further modified with a fluorophore (carboxyfluorescein, Fam) and a quencher (dabcyl, Dab) at the 5′ and 3′ termini, respectively (Figure 12). When a target strand is perfectly complementary to the SNP probe DNA oligomer, they strongly hybridise with each other, and fluorescence of Fam was observed irrespective of the presence or absence of Hg^{2+}. By contrast, when a target strand contains a mismatch (SNP) with respect to the probe DNA, the target sequence and SNP probe do not hybridise strongly. As a result, upon the addition of Hg^{2+}, the SNP probe dissociated from the target sequence and folded into a unimolecular hairpin structure through T–Hg^{II}–T base-pairing, resulting in quenching of the Fam fluorescence emission because of the decreased distance between Fam (fluorophore) and Dab (quencher).

Heteroduplex analysis combined with the formation of T–Hg^{II}–T base-pairs was proposed as another approach for high-throughput detection of SNPs.[103] In the heteroduplex analysis, SNPs

were detected on the basis of the mechanism depicted in Figure 13. Other types of SNPs were detected on the basis of the similar mechanism to that depicted in Figure 13, except for the use of the formation of C–Ag^{I}–C base-pairs.[103]

2.4) Application in nanomachines

As emerging applications of T–Hg^{II}–T and C–Ag^{I}–C base-pairs, these metallo-base-pairs were applied in nanomachines in the field of nanotechnology.[14,15] A prototype of such an application is an allosteric DNAzyme that is activated by T–Hg^{II}–T base-pairing, which is also used as a Hg^{2+} sensor with signal amplification (Figure 10).[104] Nanomachines (DNA machines) were then generated, such as DNA tweezers (automaton/memory devices),[105] DNA walkers,[106] cascade DNAzyme-reaction systems,[107-109] and logic gates.[110]

With regard to DNA tweezers, Hg^{2+} closes the DNA tweezer molecule through the hybridisation of an additional DNA strand upon T–Hg^{II}–T base-pairing.[105] It was suggested that this DNA tweezer was able to be used as an automaton and memory device.[105] With regard to the DNA walker, Hg^{2+} altered its hybridisation site on the DNA-rail molecule upon T–Hg^{II}–T base-pairing.[106] For the cascade DNAzyme-reaction systems, artificial signal transduction/amplification systems were built up from two successive DNAzyme reactions.[107-109] These cascade reaction systems consist of a ligase-like or a nuclease-like DNAzyme for the first step and horseradish-peroxidase-mimicking DNAzymes for the second step.[107-109] In these systems, Hg^{2+}/Ag^{+} activates the first step (ligase- or nuclease-like DNAzymes) by T–Hg^{II}–T/C–Ag^{I}–C base-pairing.[107-109] Lastly, logic gates (AND/OR operators) were generated by using T–Hg^{II}–T and/or C–Ag^{I}–C base-pairing (see section 2.6 for details).[110]

2.5) Conductivity of metallo-base-pairs

Long metal arrays that can be generated in metallo-DNA duplexes are suggested to be conductive.[8,10,12,13] For this reason, the charge-transport ability of metallo-base-pairs was studied in terms of hole-transport ability[89,111-113] and conductivity[114-116]. Although the conductivity and electron-transport ability of M-DNA have been reported,[41,42,114] the structure of the M-DNA molecule has not yet been determined. Therefore, the origin of its conductivity remains unknown. Currently, the conductivities of the T–Hg^{II}–T and H–Cu^{II}–H base-pairs were reported to be similar to those of semiconductors.[115,116] However, their conductivities are still worth exploring, since T–Hg^{II}–T and H–Cu^{II}–H base-pairs have been chemically and structurally well characterised. The frontier orbital of the stacked H–Cu^{II}–H base-pairs possesses a node between planes of stacked base-pairs,[117] whereas the LUMO of the T–Hg^{II}–T base-pair is continuous, covering the tandemly aligned Hg^{II}.[86] Therefore, we predicted that the T–Hg^{II}–T base-pair should be an electron acceptor;[17b,22] this was observed experimentally through fluorescence quenching by electron transfer to the T–Hg^{II}–T base-pair[118].

The generation of metal arrays in DNA molecules could be an efficient strategy for the conversion of DNA duplexes into conductive DNA nano-wires.[10,13] Currently, 10 contiguous

metallo-base-pairs have been generated by using S–Cu^{II}–S base-pairs and mixed S–Cu^{II}–S/T–Hg^{II}–T base-pairs.[119,120] The number of contiguous metallo-base-pairs for these and other base-pairs are listed in Table 6.[4,6,19,21,34119-122] Relatively long tracts of the metallo-base-pairs formed before (Table 6) indicated that tandem alignments of the metallo-base-pairs might be also thermodynamically favourable similarly as in the case of the T–Hg^{II}–T base-pairs. Therefore, detailed thermodynamic analyses of other so far uncharacterized metallo-base-pairs can be recommended to unveil how favourable these tandem alignments are. In any case, trials to make long tracts of metallo-base-pairs may provide conductive nanowires.

2.6) Response to enzymes

Several artificial base-pairs have been reported to be recognised by DNA polymerases.[123-127] Can metallo-base-pairs also be recognised? In 2010, DNA polymerases were shown, for the first time, to incorporate metallo-base-pairs in a primer-extension reaction.[128] In this experiment, dTTP was incorporated into the site opposite to thymine residues in the template strand by DNA polymerases in the presence of Hg^{2+} ions (Figure 14).[128]

More precisely, in the presence of dGTP, dCTP, and dTTP, and in the absence of Hg^{2+} ions, the primer-extension reaction with the Klenow fragment (KF) stalled at the 19-mer site just before the thymine residue (20-mer site) in the template strand. However, upon the addition of Hg^{2+} ions (10–100 μM), the enzyme read through the 20-mer site to afford the full-length 24-mer. Without dTTP, the enzyme was unable to read through the 20-mer site even in the presence of Hg^{2+} ions. MALDI-TOF mass analysis of the full-length product demonstrated the incorporation of the thymine base at the 20-mer site (Figure 15). This reaction is highly specific to Hg^{2+} ions; other metal ions, such as Mn^{2+}, Fe^{2+}, Fe^{3+}, Co^{2+}, Cu^{2+}, Zn^{2+}, Pb^{2+}, Ni^{2+}, and Au^{+}, did not promote the extension. Other polymerases, such as Taq DNA polymerase and KOD Dash DNA polymerase, also catalyse the incorporation of dTTP opposite to thymine in the template in the presence of Hg^{2+} ions.

The logical next question is whether the C–Ag^{I}–C base-pair can be used as a W–C base-pair analogue in the extension reaction catalysed by DNA polymerases. Primer-extension reactions in the presence of Ag^{+} ions (Figure 16) showed that KF unexpectedly incorporated dATP instead of dCTP into the site opposite to cytosine in the template to form an Ag^{I}-mediated C–A base-pair (C–Ag^{I}–A).[129] The structure of the C–Ag^{I}–A base-pair was tentatively assumed to contain an N3(C)–Ag^{I}–N7(A) linkage (Figure 17). Extensive studies of the extension reaction in the presence of Ag^{+} ions demonstrated that the C–Ag^{I}–T base-pair is also formed by DNA polymerases (Figure 17),[130] although the Ag^{I}-mediated enzymatic incorporation of dTTP opposite to cytosine in the template is somewhat dependent of the sequence upstream of the site of incorporation. Under 10 μM deoxynucleoside-5'-triphosphates (dNTPs), 0.2 units of KF without 3'→5' exonuclease activity KF(exo-), formation of the C–Ag^{I}–C base-pair was not observed; hence, of the three Ag^{I}-mediated base-pairs shown in Figure 17, the C–Ag^{I}–C base-pair is the most difficult to be elongated by DNA polymerase.[130] Under more stringent conditions (20 μM dCTP, 0.8 units of KF(exo-)), however, the enzymatic incorporation of dCTP opposite to cytosine in the template proceeded, depending on the

sequence of the template.[130] It was reported that 5-methyldeoxycytidine triphosphate (m^5dCTP) shows a higher substrate activity for DNA polymerase than dCTP.[131] The enzymatic formation of the T–Hg^{II}–T and C–Ag^{I}–T base-pairs is strictly governed by the Hg^{2+} and Ag^{+} ions and is also highly specific for these metal ions. Based on the high specificity and using the primed template shown in Figure 18, the regulated incorporation of Hg^{2+} and Ag^{+} ions into programmed sites in a duplex by DNA polymerase was achieved.[130]

The formation of T–Hg^{II}–T and C–Ag^{I}–C base-pairs was exploited for the construction of DNA-based logic gates.[110] Primed templates with a T–T or C–C mismatch at the 3′ primer terminus were constructed. These primed templates were amplified by the addition of Hg^{2+} and/or Ag^{+} ions. An AND gate proceeded exponential polymerase chain reaction (PCR) amplification (output) when both Hg^{2+} and Ag^{+} ions were added as inputs; the addition of either Hg^{2+} or Ag^{+} ions did not generate output signals. An OR gate proceeded exponential PCR amplification (output) in the presence of either Hg^{2+} or Ag^{+} ions or in the presence of both ions. In addition, the programmed incorporation of the T–Hg^{II}–T and C–Ag^{I}–T base-pairs, as described earlier, also behaves like an AND gate.[130]

Some artificial base-pairs have been shown to function as a “third base-pair” in PCR.[125,126] The development of replicable metallo-base-pairs composed of artificial nucleobases (metal chelators) would provide an alternative approach to the expansion of the genetic alphabet. The Dipic–Cu^{II}–Py base-pair (Figure 5) was created by Meggers, Romesberg, and Schultz with this concept in mind.[2,55,132] An actual application in this direction was first reported by Carell and coworkers. They reported a S–Cu^{II}–S base-pair as a base-pair orthogonal to natural ones (Figures 6 and 19).[56] Two opposing salicylic aldehyde deoxyribosides (dS) in a duplex form a reversible cross-link through an ethylenediamine bridge; the resulting bridge is stabilised by the coordination of a Cu^{2+} ion. This Cu^{II}-mediated artificial base-pair was recognised by DNA polymerases such as *Bst Pol I*, which selectively incorporated dSTP opposite to a templating dS base in the presence of ethylenediamine and Cu^{2+} ions. Furthermore, natural dNTPs did not compete with dSTP for binding opposite to the templating dS, so that the S–Cu^{II}–S base-pair is fully orthogonal to the canonical base-pairs, even in amplification by PCR.

A metal-mediated hetero-base-pair (metallo-base-pair composed of two different metal chelators) may be advantageous for increasing the number of codons. Most recently, the Cu^{II}-mediated hetero-base-pair purine-2,6-dicarboxylate–Cu^{II}–3-pyridine (Pur^{DC}–Cu^{II}–3-Py) was reported (Figure 20).[133] Duplexes containing this base-pair were selectively stabilised by the addition of Cu^{2+} or Zn^{2+} ions. Most of the DNA polymerases tested in the study[133] incorporated $dPur^{DC}$ triphosphate ($dPur^{DC}$TP) opposite to 3-Py in the template in the presence of Cu^{2+} ions; some polymerases incorporated $dPur^{DC}$TP even in the presence of Zn^{2+} ions. Although the enzymatic incorporation of $dPur^{DC}$ opposite to 3-Py in the template in the presence of canonical dNTPs was not described, the introduction of these artificial bases into the sites complementary to the canonical bases caused significant destabilisation of the duplexes. This may suggest that $dPur^{DC}$ and 3-Py do not compete with the natural bases in the DNA-polymerase-catalysed extension reaction.

These results suggest that a metal-mediated base-pair, formed by DNA polymerases, would be useful and widely applicable to molecular devices such as initiators for PCR amplification leading to DNA logic gates, highly sensitive metal-ion sensors,[134] and a "third base-pair" for expanding the genetic alphabet.

3) Summary and perspectives

In this feature article, we dealt with both natural-nucleobase-based metallo-base-pairs and artificial metal-chelator-based ones. First, we summarize a current status of natural-nucleobase-based metallo-base-pairs as a starting point of this Feature Article. We then propose future prospects of the metallo-base-pairs (natural-base-based and artificial metal-chelator-based ones) on the basis of their accumulated fundamental properties.

Since we discovered T–Hg^{II}–T and C–Ag^{I}–C base-pairs, we have extensively explored their fundamental properties. To date, we determined the chemical structure of the T–Hg^{II}–T base-pair based on the observation of $^{2}J(^{15}N,^{15}N)$ in ^{15}N NMR spectra, which is solid evidence for the N3–Hg^{II}–N3 linkage. Additionally, we determined the 3D structures of DNA duplexes including tandem T–Hg^{II}–T base-pairs in solution and in the crystal. Unexpectedly, the ^{15}N NMR spectra (downfield shift of N3 at the Hg^{II}-ligated site) and the Raman spectra (low-wavenumber shift of the C4=O4 stretching) indicated the highly ionic nature of the N3–Hg^{II} bond, although it has covalent nature. Theoretical calculations confirmed the low covalency of the N3–Hg^{II} bond (a lowered bond order (0.22) compared to the original N3-H bond (0.50) of thymine) and the resulting highly cationic nature of the Hg^{II}. Furthermore, ^{15}N NMR parameters ($^{2}J(^{15}N,^{15}N)$ and ^{15}N chemical shifts) derived from T–Hg^{II}–T base-pairs have become standard reference values for NMR parameters for N-metallated compounds. This means that our NMR spectroscopic parameters have influenced coordination and inorganic chemistry, and they will form the structural/chemical basis for later studies.

We further determined the thermodynamic parameters for T–Hg^{II}–T and C–Ag^{I}–C base-pairing. In both cases, ITC studies gave negative enthalpy values and positive entropy values for their formations. The positive entropy change was demonstrated to be a dehydration entropy, as the dehydration of Hg^{2+} ions was demonstrated by the 3D structures of metallo(Hg^{II})-DNA duplexes. This is quite a rare case for which the structurally silent entropy parameter was identified from a 3D structure.

The 3D structures further demonstrated the close contact between Hg^{II} in adjacent T–Hg^{II}–T base-pairs in DNA duplexes. This Hg^{II}–Hg^{II} close contact provides evidence for the metallophilic attraction, which was also indicated by our theoretical calculations on tandem T–Hg^{II}–T (U–Hg^{II}–U) base-pairs. Thus, all of the experimental and theoretical data consistently explain the fundamental physicochemical properties of the T–Hg^{II}–T base-pair, and these properties were comprehensively characterised through basic structural, spectroscopic, thermodynamic, and theoretical studies. Therefore, as the next targets, the chemical structures of C–Ag^{I}–C/C–Ag^{I}–A/C–Ag^{I}–T base-pairs and their 3D structures in DNA duplexes should be

determined to generate a complete fundamental dataset for metallo-base-pairs composed of natural nucleobases.

As a future prospect, metallo-DNA duplexes with a long tract of metallo-base-pairs may be assumed attractive with regard to construction of conductive nanowires and semiconductors. Nevertheless, it still remains unclear whether such a long tract of metallo-base-pairs can be generated because growing repulsion among metal cations may be destructive for 3D structure. For this issue, the crystal structure of the metallo(Hg^{II})-DNA duplex unveiled the close distance between Hg^{2+} ions (3.3 Å) of neighbouring T–Hg^{II}–T base-pairs.[23] Furthermore, the positive cooperativity for Hg^{II}-binding to the consecutive T–T mismatches (second K_a > first K_a, Table 5) indicated that the close contact of Hg^{2+} ions is thermodynamically favourable. Hence, the key issue to be resolved is how to produce a metallo-DNA duplex long enough for construction of functional nanowire. In addition, their conductivities must be examined. In that regard, theoretical implication of a continuous (node-free) LUMO overlap through adjacent Hg^{2+} ions indicated that effective route for excess electrons may exist. Both the structural and the electronic properties of metallo(Hg^{II})-DNA thus suggest that realization of a conductive nanowire is possible.

Artificial metal-chelator-based metallo-base-pairs are also interesting candidates of a conductive nanowire. Their several 3D structures are available (Dipic–Cu^{II}–Py[55], S−Cu^{II}−S[56], H−Cu^{II}−H[58], C−Au^{III}−G[60] and Im−Ag^{I}−Im[19,21]), and electronic properties of the Im-Ag^{I}-Im base-pair were studied[21]. It is also noteworthy that the longest metal-arrays were produced using the S-Cu^{II}-S base pair and S-Cu^{II}-S/T-Hg^{II}-T mixed base pairs,[119,120] In addition, fine-tuning or drastic alteration of the properties of metal-chelator-based metallo-DNA molecules can be freely performed by modifying or altering molecular skeletons. On the other hand, natural nucleobases-based metallo-DNAs may have some limitations for their applications into molecular devices, due to their limited chemical diversities of nucleobases even if metallo-DNAs with modified nucleobases[70,71] are taken into considerations. However, extensively accumulated structural/physicochemical data of T-Hg^{II}-T and C-Ag^{I}-C base-pairs might help us construct molecular devices based on their physicochemical properties.

Therefore, metallo-DNA molecules with other existing metallo-base pairs (artificial metal-chelator-based and natural nucleobases-based ones) need to be characterized both structurally and physicochemically toward their technological applications. We may foresee that the number of structures and spectroscopic/thermodynamic parameters of metallo-DNA molecules will increase due to their necessity for the construction of the molecular devices based on the bottom-up approach. Such fundamental achievements will lead to the rational design of variety of new molecular nanodevices in future.

Acknowledgements

This work was supported by Grants-in-aid for Scientific Research (A) (24245037 to A.O., J.K., H.U., H.T., and Y.T.), (B) (24310163 to Y.T.) and Challenging Exploratory Research (15K13734 to Y.T.) from the Ministry of Education, Culture, Sports, Science and Technology (MEXT), Japan; a Human

Frontier Science Program (HFSP) Young Investigator Grant from HFSPO, France (Y.T. and V.S.); and GAČR (P205/10/0228 and 15-21387S to V.S.) from the Czech Republic. T.D. and K.F. are the recipients of a Research Fellowship for Young Scientists from the Japan Society for the Promotion of Science (JSPS). Y.T. and V.S. were further supported by an Invitation Fellowship for Research in Japan (Short-Term) from JSPS.

Notes and references

[a] Faculty of Pharmaceutical Sciences, Tokushima Bunri University, 180 Nishihama-Boji, Yamashirocho, Tokushima, Tokushima 980-8578, Japan. E-mail: tanakay@ph.bunri-u.ac.jp

[b] Graduate School of Pharmaceutical Sciences, Tohoku University, 6-3 Aza-Aoba, Aramaki, Aoba-ku, Sendai, Miyagi 980-8578, Japan. E-mail: tanaka@mail.pharm.tohoku.ac.jp

[c] Department of Materials and Life Sciences, Faculty of Science and Technology, Sophia University 7-1 Kioi-cho, Chiyoda-ku, Tokyo 102-8554, Japan

[d] Institute of Organic Chemistry and Biochemistry, Academy of Sciences of the Czech Republic, v.v.i., Flemingovo náměstí 2, 16610, Praha 6, Czech Republic.

[e] Department of Material & Life Chemistry, Kanagawa University, 3-27-1 Rokkakubashi, Kanagawa-ku, Yokohama, Kanagawa 221-8686, Japan. E-mail: akiraono@kanagawa-u.ac.jp

[f] Osaka University of Pharmaceutical Sciences, 4-20-1 Nasahara, Takatsuki, Osaka 569-1094, Japan.

[g] Department of Applied Chemistry, Faculty of Science, Tokyo University of Science, 1-3 Kagurazaka, Shinjuku-ku, Tokyo 162-8601, Japan.

† Electronic Supplementary Information (ESI) available: Chemical structures of metallo-base-pairs and their references. See DOI: 10.1039/c0xx00000x/

1. K. Tanaka and M. Shionoya, *J. Org. Chem.* 1999, **64**, 5002-5003.
2. E. Meggers, P. L. Holland, W. B. Tolman, F. E. Romesberg and P. G. Schultz, *J. Am. Chem. Soc.*, 2000, **122**, 10714-10715.
3. K. Tanaka, A. Tengeiji, T. Kato, N. Toyama, M. Shiro and M. Shionoya, *J. Am. Chem. Soc.*, 2002, **124**, 12494-12498.
4. K. Tanaka, A. Tengeiji, T. Kato, N. Toyama and M. Shionoya, *Science*, 2003, **299**, 1212-1213.
5. A. Ono and H. Togashi, *Angew. Chem.*, 2004, **116**, 4400-4402; *Angew. Chem. Int. Ed.*, 2004, **43**, 4300-4303.
6. Y. Miyake, H. Togashi, M. Tashiro, H. Yamaguchi, S. Oda, M. Kudo, Y. Tanaka, Y. Kondo, R. Sawa, T. Fujimoto, T. Machinami and A. Ono, *J. Am. Chem. Soc.*, 2006, **128**, 2172-2173.
7. A. Ono, S. Cao, H. Togashi, M. Tashiro, T. Fujimoto, T. Machinami, S. Oda, Y. Miyake, I. Okamoto and Y. Tanaka, *Chem. Commun.*, 2008, 4825-4827.
8. T. Carell, C. Behrens and J. Gierlich, *Org. Biomol. Chem.*, 2003, **1**, 2221-2228.
9. H.-A. Wagenknecht, *Angew. Chem.*, 2003, **115**, 3322-3324; *Angew. Chem. Int. Ed.*, 2003, **42**, 3204-3206.

10. G. H. Clever, C. Kaul and T. Carell, *Angew. Chem.* 2007, **119**,6340-6350; *Angew. Chem. Int. Ed.*, 2007, **46**, 6226-6236.
11. A. Ono, H. Torigoe, Y. Tanaka and I. Okamoto, *Chem. Soc. Rev.*, 2011, **40**, 5855-5866..
12. Y. Takezawa and M. Shionoya, *Acc. Chem. Res.*, 2012, **45**, 2066-2076.
13. P. Scharf and J. Müller, *ChemPlusChem*, 2013, **78**, 20-34.
14. X. Liu, C.-H. Lu and I. Willner, *Acc. Chem. Res.*, 2014, **47**, 1673-1680.
15. F. Wang, C.-H. Lu and I. Willner, *Chem. Rev.*, 2014, **114**, 2881-2941.
16. Y. Tanaka, S. Oda, H. Yamaguchi, Y. Kondo, C. Kojima and A. Ono, *J. Am. Chem. Soc.*, 2007, **129**, 244-245.
17. (a) Y. Tanaka and A. Ono, *Dalton Trans.*, 2008, 4965-4974; (b) Y. Tanaka and A. Ono, in *Metal Complexes - DNA Interactions,* ed. N. Hadjiliadis and E. Sletten, John Wiley & Sons, 2009, pp. 439-462..
18. T. Dairaku, K. Furuita, H. Sato, J. Šebera, D. Yamanaka, H. Otaki, S. Kikkawa, Y. Kondo, R. Katahira, F. M. Bickelhaupt, C. F. Guerra, A. Ono, V. Sychrovský, C. Kojima, and Y. Tanaka, *Chem. Commun.*, 2015, **51**, 8488-8491.
19. S. Johannsen, N. Megger, D. Böhme, R. K. O. Sigel and J. Müller, *Nat. Chem.*, 2010, **2**, 229-234.
20. T. Uchiyama, T. Miura, H. Takeuchi, T. Dairaku, T. Komuro, T. Kawamura, Y. Kondo, L. Benda, V. Sychrovský, P. Bouř, I. Okamoto, A. Ono and Y. Tanaka, *Nucleic Acids Res.*, 2012, **40**, 5766-5774.
21. S. Kumbhar, S. Johannsen, R. K. O. Sigel, M. P. Waller and J. Müller, *J. Inorg. Biochem.*, 2013, **127**, 203-210.
22. H. Yamaguchi, J. Šebera, J. Kondo, S. Oda, T. Komuro, T. Kawamura, T. Daraku, Y. Kondo, I. Okamoto, A. Ono, J. V. Burda, C. Kojima, V. Sychrovský and Y. Tanaka, *Nucleic Acids Res.*, 2014, **42**, 4094-4099.
23. J. Kondo, T. Yamada, C. Hirose, I. Okamoto, Y. Tanaka and A. Ono, *Angew. Chem.*, 2014, **126**, 2417-2420; *Angew. Chem. Int. Ed.*, 2014 **53**, 2385-2388.
24. R. W. Chrisman, S. Mansy, H. J. Peresie, A. Ranade, T. A. Berg and R. S. Tobias, *Bioinorg. Chem.*, 1977, **7**, 245-266.
25. B. Morzyk-Ociepa and D. Michalska, *J. Mol. Struct.*, 2001, **598**, 133-144.
26. D. W. Gruenwedel, M. K. Cruikshank and G. M. Smith, *J. Inorg. Biochem.*, 1993, **52**, 251-261.
27. Y. Tanaka, H. Yamaguchi, S. Oda, M. Nomura, C. Kojima, Y. Kondo and A. Ono, *Nucleosides Nucleotides Nucleic Acids*, 2006, **25**, 613-624.
28. D. W. Gruenwedel, *J. Inorg. Biochem.*, 1994, **56**, 201-212.
29. D. W. Gruenwedel, *Biophys. Chem.*, 1994, **52**, 115.
30. (a) E. Buncel, C. Boone, H. Joly, R. Kumar and A. R. Norris, *J. Inorg. Biochem.*, 1985, **25**, 61-73; (b) E. Buncel, C. Boone and H. Joly, *Inorg. Chim. Acta*, 1986, **125**, 167-172. (c) A. R. Norris and R. Kumar, *Inorg. Chim. Acta*, 1984, **93**, 33–35.

31. Z. Kuklenyik and L. G. Marzilli, *Inorg. Chem.*, 1996, **35**, 5654-5662.
32. (a) S. Katz, *J. Am. Chem. Soc.*, 1952, **74**, 2238-2245; (b) C. A. Thomas, *J. Am. Chem. Soc.*, 1954, **76**, 6032-6034; (c) W. F. Dove and T. Yamane, *Biochem. Biophys. Res. Commun.*, 1960, **3**, 608-612; (d) T. Yamane and N. Davidson, *J. Am. Chem. Soc.*, 1961, **83**, 2599-2607 (e) S. Katz, *Nature*, 1962, **194**, 569; (f) S. Katz, *Nature*, 1962, **195**, 997; (g) T. Yamane and N. Davidson, *Biochim. Biophys. Acta*, 1962, **55**, 780-782; (h) S. Katz, *Biochim. Biophys. Acta*, 1963, **68**, 240.
33. P. R. Young, U. S. Nandi and N. R. Kallenbach, *Biochemistry*, 1982, **21**, 62-66.
34. S. Johannsen, S. Paulus, N. Düpre, J. Müller and R. K. O. Sigel, *J. Inorg. Biochem.*, 2008, **102**, 1141-1151.
35. N. Å. Frøystein and E. Sletten, *J. Am. Chem. Soc.*, 1994, **116**, 3240-3250.
36. S. Steinkopf, W. Nerdal, A. Kolstad and E. Sletten, *Acta Chem. Scand.*, 1996, **50**, 775-782.
37. E. Sletten and N. Å. Frøystein, in *Metal Ions in Biological Systems*, *Vol 32*, ed. A. Sigel and H. Sigel, Marcel Dekker, 1996, pp397-418.
38. E. Sletten and W. Nerdal, in *Metal Ions in Biological Systems*, ed. A. Sigel and H. Sigel, Marcel Dekker, *Vol 34*, 1997, pp 479-500.
39. B. Morzyk-Ociepa and D. Michalska, *Spectrochim. Acta A*, 2003, **59**, 1247-1254.
40. J. S. Lee, L. J. P. Latimer and R. S. Reid, *Biochem. Cell Biol.*, 1993, **71**, 162-168.
41. P. Aich, S. L. Labiuk, L. W. Tari, L. J. T. Delbaere, W. J. Roesler, K. J. Falk, R. P. Steer and J. S. Lee, *J. Mol. Biol.*, 1999, **294**, 477-485.
42. P. Aich, R. J. S. Skinner, S. D. Wettig, R. P. Steer and J. S. Lee, *J. Biomol. Struct. Dyn.*, 2002, **20**, 93-98.
43. E. C. Fusch and B. Lippert, *J. Am. Chem. Soc.*, 1994, **116**, 7204-7209.
44. S. S. Alexandre, J. M. Soler, L. Seijo and F. Zamora, *Phys. Rev. B*, 2006, **73**, 205112.
45. D. A. Megger and J. Müller, *Nucleosides Nucleotides Nucleic Acids*, 2010, **29**, 27-38.
46. H. A. Day, C. Huguin and Z. A. E. Waller, *Chem. Commun.*, 2013, **49**, 7696-7698.
47. M. Berdakin, V. Steinmetz, P. Maitre and G. A. Pino, *J. Phys. Chem. A*, 2014, **118**, 3804-3809.
48. I. Goncharova, *Spectrochim Acta A*. 2014 **118**, 221-227.
49. S. S. Mallajosyula and S. K. Pati, *Angew. Chem.*, 2009, **121,** 5077-5081; *Angew. Chem. Int. Ed.*, 2009, **48**, 4977-4981.
50. G. W. Buchanan and J. B. Stothers, *Can. J. Chem.*, 1982, **60**, 787-791.
51. G. W. Buchanan and M. J. Bell, *Can. J. Chem.*, 1983, **61**, 2445-2448.
52. Y. Tanaka, C. Kojima, E. H. Morita, Y. Kasai, K. Yamasaki, A. Ono, M. Kainosho and K. Taira, *J. Am. Chem. Soc.*, 2002, **124**, 4595-4601.
53. G. Wang, B. L. Gaffney and R. A. Jones, *J. Am. Chem. Soc.*, 2004, **126**, 8908-8909.
54. Y. Tanaka and K. Taira, *Chem. Commun.*, 2005, 2069-2079.
55. S. Atwell, E. Meggers, G. Spraggon and P. G. Schultz, *J. Am. Chem. Soc.*, 2001, **123**, 12364-12367.
56. C. Kaul, M. Müller, M. Wagner, S. Schneider and T. Carell, *Nat. Chem.*, 2011, **3**, 79-8004.

57. G. H. Clever, K. Polborn, T. Carell, *Angew. Chem.* 2005, **117**, 7370-7374; *Angew. Chem. Int. Ed.* 2005, **44**, 7204-7208.
58. M. K. Schlegel, L.-O. Essen and E. Meggers, *J. Am. Chem. Soc*., 2008, **130**, 8158-8159.
59. L.E. Orgel, *Trends Biochem. Sci*., 1998, **23**, 491-495.
60. E. Ennifar, P. Walter and P. Dumas, *Nucleic Acids Res*., 2003, **31**, 2671-2682.
61. L. D. Kosturko, C. Folzer and R. F. Stewart, *Biochemistry*, 1974, **13**, 3949-3952.
62. H. Torigoe, A. Ono and T. Kozasa, *Chem. Eur. J.*, 2010, **16**, 13218-13225.
63. H. Torigoe, I. Okamoto, T. Dairaku, Y. Tanaka, A. Ono and T. Kozasa, *Biochimie*, 2012, **94**, 2431-2440.
64. J. Šebera, J. Burda, M. Straka, A. Ono, C. Kojima, Y. Tanaka and V. Sychrovský, *Chem. Eur. J.*, 2013, **19**, 9884-9894.
65. K. Petrovec, B. J. Ravoo and J. Müller, *Chem. Commun.*, 2012, **48**, 11844-11846.
66. H. Torigoe, Y. Miyakawa, A. Ono and T. Kozasa, *Thermochimica Acta*, 2012, **532**, 28-35.
67. H. Torigoe, Y. Miyakawa, A. Ono and T. Kozasa, *Nucleosides Nucleotides Nucleic Acids*, 2011, **30**, 149-167.
68. P. Pyykkö, *Chem. Rev.*, 1997, **97**, 597-636..
69. P. Pyykkö and M. Straka, *Phys. Chem. Chem. Phys.*, 2000, **2**, 2489-2493.
70. I. Okamoto, K. Iwamoto, Y. Watanabe, Y. Miyake and A. Ono, *Angew. Chem. Int. Ed.*, 2009, **48**, 1648-8320.
71. I. Okamoto, T. Ono, R. Sameshima and A. Ono, *Chem. Commun.*, 2012, **48**, 4347-4349.
72. A. Bagno and G. Saielli, *J. Am. Chem. Soc.*, 2007, **129**, 11360-1361.
73. L. Benda, M. Straka, V. Sychrovský, P. Bouř and Y. Tanaka, *J. Phys. Chem. A*, 2012, **116**, 8313.
74. H. Miyachi, T. Matsui, Y. Shigeta and K. Hirao, *Phys. Chem. Chem. Phys.*, 2010, **12**, 909.
75. J. Müller, D. Böhme, P. Lax, M. M. Cerdà and M. Roitzsch, *Chem. Eur. J.*, 2005, **11**, 6246-6253.
76. D. A. Megger, C. Fonseca Guerra, J. Hoffmann, B. Brutschy, F. M. Bickelhaupt and J. Müller, *Chem. Eur. J.*, 2011, **17**, 6533-6544.
77. T. Marino, N. Russo, M. Toscano and M. Pavelka, *Dalton Trans.*, 2012, **41**, 1816-1823
78. T. Matsui, H. Miyachi, Y. Nakanishi, Y. Shigeta, T. Sato, Y. Kitagawa, M. Okumura and K. Hirao, *J. Phys. Chem. B*, 2009, **113**, 12790-12795.
79. H. Miyachi, T. Matsui, Y. Shigeta, K. Yamashita and K. Hirao, *Chem. Phys. Lett.*, 2010, **495**, 125-130.
80. L. Benda, M. Straka, Y. Tanaka and V. Sychrovský, *Phys. Chem. Chem. Phys.*, 2011, **13**, 100-103.
81. M. Kauch and M. Pecul, *ChemPhysChem*, 2012, **13**, 1332-1338; *ChemPhysChem*, 2012, **13**, 2627.
82. S. S. Mallajosyula and S. K. Pati, *J. Phys. Chem. Lett.*, 2010, **1**, 1881-1894.
83. J. Zhao, L. Han, H. Yang, J. Liu and Y. Bu, *ChemPhysChem*, 2012, **13**, 3293-3302.

84. P. K. Samanta and S. K. Pati, *Chem. Eur. J.*, 2014, **20**, 1760-1764.
85. P. K. Samanta, A. K. Manna and S. K. Pati, *Chem. Asian J.*, 2012, **7**, 2718-2728.
86. A. A. Voityuk, *J. Phys. Chem. B*, 2006, **110**, 21010-21013.
87. H. Liu, G. Q. Li, H. Ai, J. Li and Y. Bu, *J. Phys. Chem. C*, 2011, **115**, 22547-22556.
88. Y. Nakanishi, T. Matsui, Y. Kitagawa, Y. Shigeta, T. Saito, Y. Kataoka, T. Kawakami, M. Okumura and K. Yamaguchi, *Bull. Chem. Soc. Japan*, 2011, **84**, 366-375.
89. I. Kratochvílová, M. Golan, M. Vala, M. Špérová, M. Weiter, O. Páv, J. Šebera, I. Rosenberg, V. Sychrovský, Y. Tanaka and F. M. Bickelhaupt, *J. Phys. Chem. B*, 2014, **118**, 5374-5381.
90. P. D. Selid, H. Y. Xu, E. M. Collins, M. S. Face-Collins and J. X. Zhao, *Sensors*, 2009, **9**, 5446-5459.
91. G. Aragay, J. Pons and A. Merkoçi, *Chem. Rev.*, 2011, **111**, 3433-3458.
92. D. L. Ma, D. S.-H. Chan, B. Y.-W. Man and C.-H. Leung, *Chem. Asian J.*, 2011, **6**, 986-1003.
93. M. Li, H. Gou, I. Al-Ogaidi and N. Wu, *ACS Sustain. Chem. Engineer.*, 2013, **1**, 713-723.
94. D.-L. Ma, H.-Z. He, K.-H. Leung, H.-J. Zhong, D. S.-H. Chan and C.-H. Leung, *Chem. Soc. Rev.*, 2013, **42**, 3427-3440.
95. X. Liu, C. Qi, T. Bing, X. Cheng and D. Shangguan, *Talanta*, 2009, **78**, 253-258.
96. Y.S. Wang, C.-C. Cheng, J.-K. Chen, F.-H. Ko and F.-C. Chang, *J. Materials Chem. A*, 2013, **1**, 7745-7750.
97. N. Dave, M. Y. Chan, P.-J. J. Huang, B. D. Smith and J. Liu, *J. Am. Chem. Soc.*, 2010, **132**, 12668-12673.
98. P.-J. J. Huang and J. Liu, *Chem. Eur. J.*, 2011, **17**, 5004-5010.
99. Y. Yu, B. W. Zhang, M. Yu, B. Deng, L. F. Li, C. H. Fan and J. Y. Li, *Sci. China Chem.*, 2012, **55**, 2202-2208.
100. M. Kuriyama, K. Haruta, T. Dairaku, T. Kawamura, S. Kikkawa, K. Inamoto, H. Tsukamoto, Y. Kondo, H. Torigoe, I. Okamoto, A. Ono, E. H. Morita, and Y. Tanaka, *Chem. Pharm. Bull.*, 2014,**62**, 709-712.
101. D. He, X. He, K. Wang, Y. Zhao and Z. Zou, *Langmuir*, 2013, **29**, 5896-5904.
102. Y.-W. Lin, H.-T. Ho, C.-C. Huang and H.-T. Chang, *Nucleic Acids Res.*, 2008, **36**, e123.
103. H. Torigoe, A. Ono and T. Kozasa, *Transition Met. Chem.*, 2011, **36**, 131-144.
104. J. Liu and Y. Lu, *Angew. Chem.*, 2007, **119**, 7731-7734; *Angew. Chem. Int. Ed.*, 2007, **46**, 7587-7590.
105. Z.-G. Wang, J. Elbaz, F. Remacle, R. D. Levine and I. Willner, *Proc. Natl. Acad. Sci., USA*, 2010, **107**, 21996-22001.
106. Z.-G. Wang, J. Elbaz and I. Willner, *Nano Lett.*, 2011, **11**, 304-309.
107. D. Li, A. Wieckowska and I. Willner, *Angew. Chem.*, 2008, **120**, 3991-3995; *Angew. Chem. Int. Ed.*, 2008, **47**, 3927-3931.
108. S. Shimron, J. Elbaz, A. Henning and I. Willner, *Chem. Commun.*, 2010, **46**, 3250-3252.
109. F. Wang, R. Orbach and I. Willner, *Chem. Eur. J.*, 2012, **18**, 16030-16036.
110. K. S. Park, C. Jung and H. G. Park, *Angew. Chem.*, 2010, **122**, 9951-9954; *Angew. Chem. Int.*

Ed., 2010, **49**, 9757-9760.
111. T. Ito, G. Nikaido and S. I. Nishimoto, *J. Inorg. Biochem.*, 2007, **101**, 1090-1093.
112. J. Joseph and G. B. Schuster, *Org. Lett.*, 2007, **9**, 1843-1846.
113. T. Ehrenschwender, W. Schmucker, C. Wellner, T. Augenstein, P. Carl, J. Harmer, F. Breher and H.-A. Wagenknecht, *Chem. Eur. J.*, 2013, **19**, 12547-12552.
114. B. Liu, A. J. Bard, C. Z. Li and H. B. Kraatz, *J. Phys. Chem. B*, 2005, **109**, 5193-5198.
115. H. Isobe, N. Yamazaki, A. Asano, T. Fujino, W. Nakanishi and S. Seki, *Chem. Lett.*, 2011, **40**, 318-319.
116. S. Liu, G. H. Clever, Y. Takezawa, M. Kaneko, K. Tanaka, X. Guo and M. Shionoya, *Angew. Chem. Int. Ed.*, 2011, **123**, 9048-9052; *Angew. Chem. Int. Ed.*, 2011, **50**, 8886-8890.
117. H. Y. Zhang, A. Calzolari and R. Di Felice, *J. Phys. Chem. B*, 2005, **109**, 15345-15348.
118. L. Guo, N. Yin and G. Chen, *J. Phys. Chem. C*, 2011, **115**, 4837-4842.
119. K. Tanaka, G. H. Clever, Y. Takezawa, Y. Yamada, C. Kaul, M. Shionoya and T. Carell, *Nat. Nanotechnol.*, 2006, **1**, 190-194. ; see also : J. Müller, *Nature*, 2006, **444**, 698.
120. G. H. Clever and T. Carell, *Angew. Chem.*, 2007, **119**, 254-257; *Angew. Chem. Int. Ed.*, 2007, **46**, 250-253.
121. N. Zimmermann, E. Meggers and P. G. Schultz, *Bioorg. Chem.*, 2004, **32**, 13-25.
122. C. Switzer, S. Sinha, P. H. Kim and B. D. Heuberger, *Angew. Chem.*, 2005, **117**, 1553-1556; *Angew. Chem. Int. Ed.*, 2005, **44**, 1529-1532.
123. J. A. Piccirilli, T. Krauch, S. E. Moroney and S. A. Benner, *Nature*, 1990, **343**, 33-37.
124. K. M. Guckian, T. R. Krugh and E. T. Kool, *Nat. Struct. Biol.* 1998, **5**, 954-959.
125. I. Hirao, T. Mitsui, M. Kimoto and S. Yokoyama, *J. Am. Chem. Soc.*, 2007, **129**, 15549-15555.
126. D. A. Malyshev, Y. J. Seo, P. Ordoukhanian and F. E. Romesberg, *J. Am. Chem. Soc.* 2009, **131**, 14620-14621.
127. N. Minakawa, S. Ogata, M. Takahashi and A. Matsuda, *J. Am. Chem. Soc.* 2009, **131**, 1644-1645.
128. H. Urata, E. Yamaguchi, T. Funai, Y. Matsumura and S-i. Wada, *Angew. Chem.*, 2010, **122**, 6666-6669; *Angew. Chem. Int. Ed.*, 2010, **49**, 6516-6519.
129. T. Funai, Y. Miyazaki, M. Aotani, E. Yamaguchi, O. Nakagawa, S. Wada, H. Torigoe, A. Ono and H. Urata, *Angew. Chem.*, 2012, **124**, 6570-6572; *Angew. Chem. Int. Ed.*, 2012, **51**, 6464-6466.
130. T. Funai, J. Nakamura, Y. Miyazaki, R. Kiriu, O. Nakagawa, S.-i. Wada, A. Ono and H. Urata, *Angew. Chem.*, 2014, **126**, 6742-6745; *Angew. Chem. Int. Ed.*, 2014, **53**, 6624-6627.
131. T. Tian, S. Peng, H. Xiao, Y. Long, B. Fu, X. Zhang, S. Guo, S. Wang, X. Zhou, S. Liu and X. Zhou, *Chem. Commun.*, 2013, **49**, 10085-10087.
132. N. Zimmermann, E. Meggers, P. G. Schultz, *J. Am. Chem. Soc.* 2002, **124**, 13684-13685.
133. E.-K. Kim and C. Switzer, *ChemBioChem.*, 2013, **14**, 2403-2047.
134. G. Zhu, Y. Li and C.-Y. Zhang, *Chem. Commun.*, 2014, **50**, 572-574.
135. C.-K. Chiang, C.-C. Huang, C.-W. Liu and H.-T. Chang, *Anal. Chem.*, 2008, **80**, 3716-3721.

136. R. Freeman, T. Finder and I. Willner, *Angew. Chem.*, 2009, **121**, 7958; *Angew. Chem. Int. Ed.*, 2009, **48**, 7818-7821.
137. J.-S. Lee, M. S. Han and C. A. Mirkin, *Angew. Chem.*, 2007, **119**, 4171-4174; *Angew. Chem. Int. Ed.*, 2007, **46**, 4093-4096.
138. T. Li, B. Li, E. Wang and S. Dong, *Chem. Commun.*, 2009, 3551-3553.
139. K. S. Park, J. Y. Lee and H. G. Park, *Chem. Commun.*, 2012, **48**, 4549-4551.
140. G. Mor-Piperberg, R. Tel-Vered, J. Elbaz and I. Willner, *J. Am. Chem. Soc.*, 2010, **132**, 6878-6879.

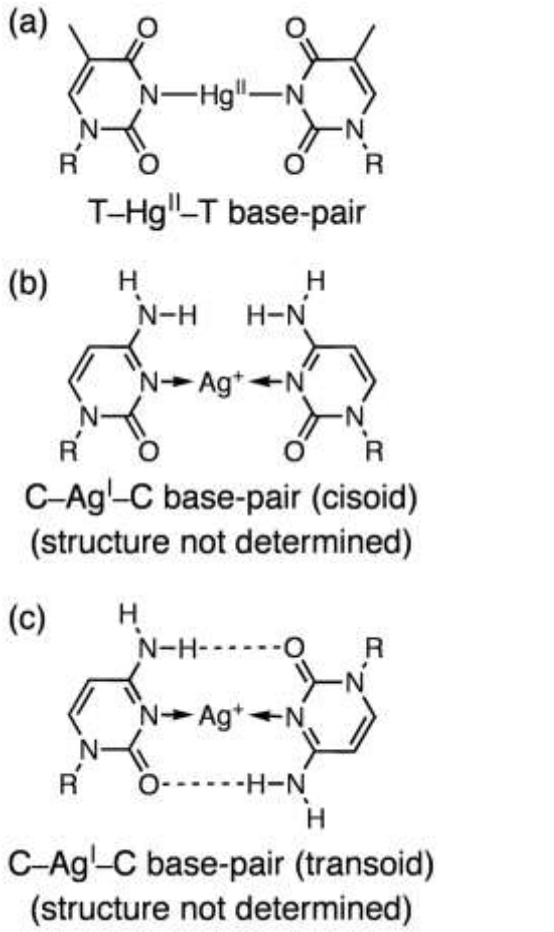

Figure 1. T–Hg^{II}–T and C–Ag^{I}–C base-pairs. R denotes ribose.

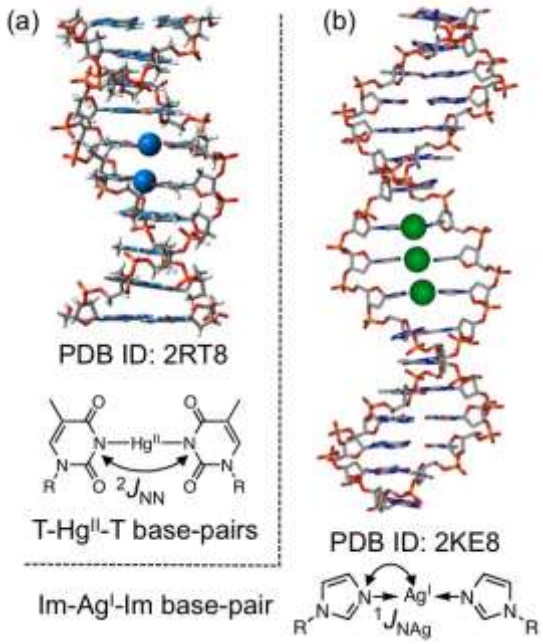

Figure 2. Three-dimensional structures of metallo-DNA molecules. R denotes ribose.

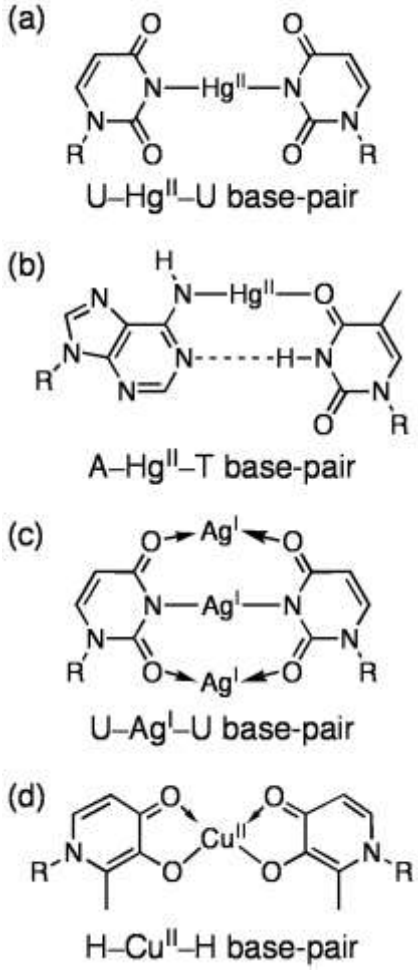

Figure 3. Structures of metallo-base-pairs studied spectroscopically. R denotes ribose.

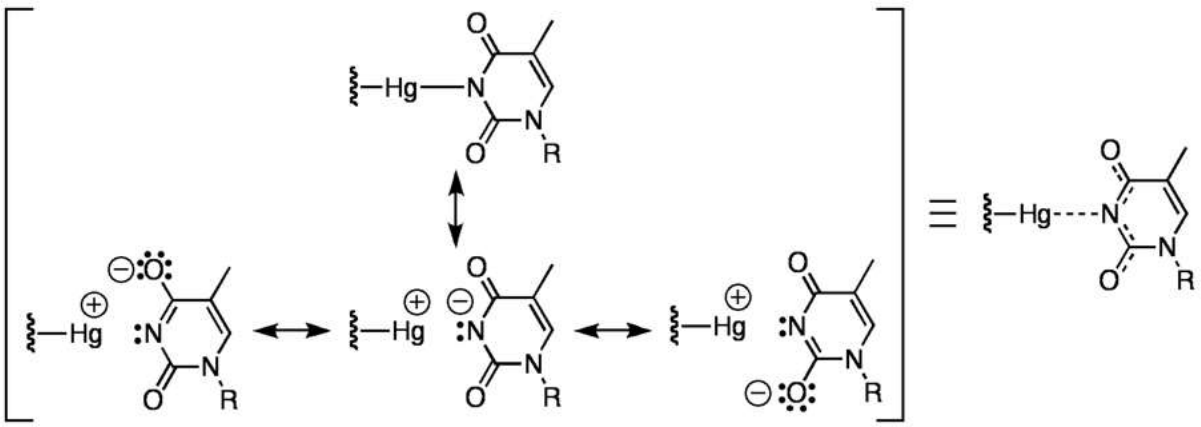

Figure 4. Resonance contributors for the T–Hg^{II}–T base-pair. R denotes ribose.

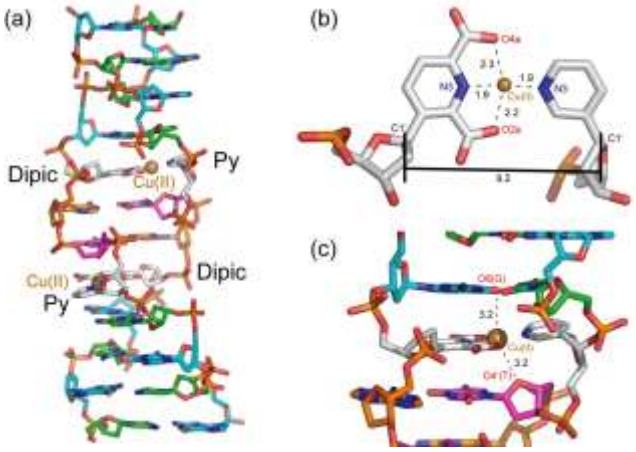

Figure 5. (a) Overall structure of the Z-form DNA duplex containing Dipic–Cu^{II}–Py base-pairs (PDB ID = 1JES).[55] (b) Detailed geometry of the Dipic–Cu^{II}–Py base-pair. The C1′–C1′ distance (Å) is indicated by a solid line, and distances (Å) between Cu^{II} and four atoms in its proximity are indicated by dashed lines, respectively. (c) Side view of the Dipic–Cu^{II}–Py base-pair. The distances (Å) between Cu^{II} in Dipic–Cu^{II}–Py base-pair and O6(G) and O4'(T) atoms in neighbouring base-pairs are indicated by red dashed lines (distances in Å).

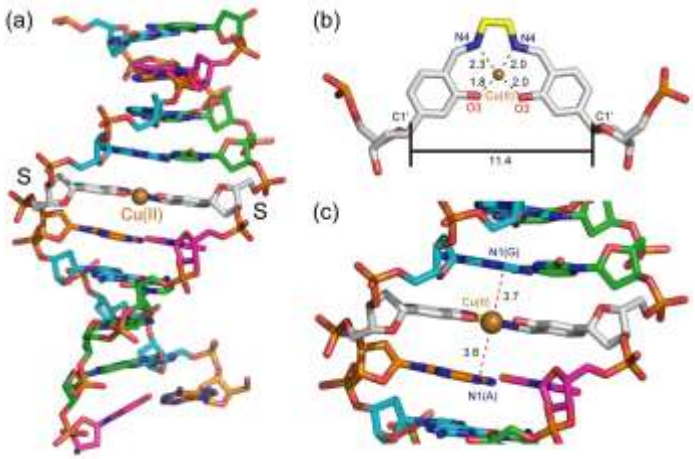

Figure 6. (a) Overall structure of the B-form DNA duplex containing an S–Cu^{II}–S base-pair (PDB ID = 2XY5).[56] (b) Detailed geometry of the S–Cu^{II}–S base-pair. The C1′–C1′ distanc (Å) is represented by a solid line, and critical distances (Å) with Cu^{II} are shown with dashed lines. (c) Side view of the S–Cu^{II}–S base-pair. Axial interactions are represented by red dashed lines (distances in Å).

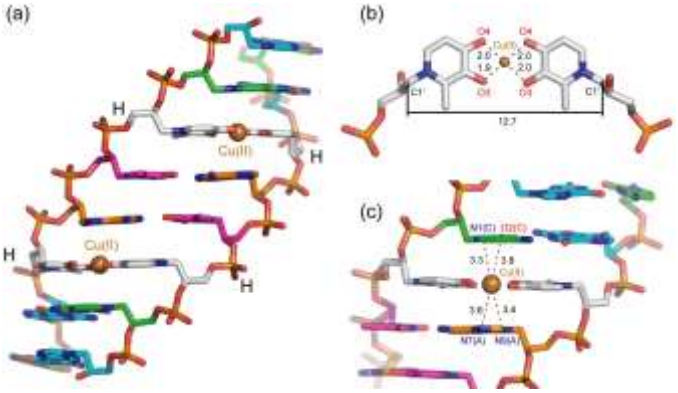

Figure 7. (a) Overall structure of the GNA (glycol nucleic acid) duplex containing an H–Cu^{II}–H base-pair (PDB ID = 1JAA).[58] (b) Detailed geometry of the H–Cu^{II}–H base-pair. The C1′–C1′ distanc (Å) is represented by a solid line, and critical distances (Å) with Cu^{II} are shown with dashed lines. (c) Side view of the H–Cu^{II}–H base-pair. Interactions toward axial directions are represented by red dashed lines (distances in Å).

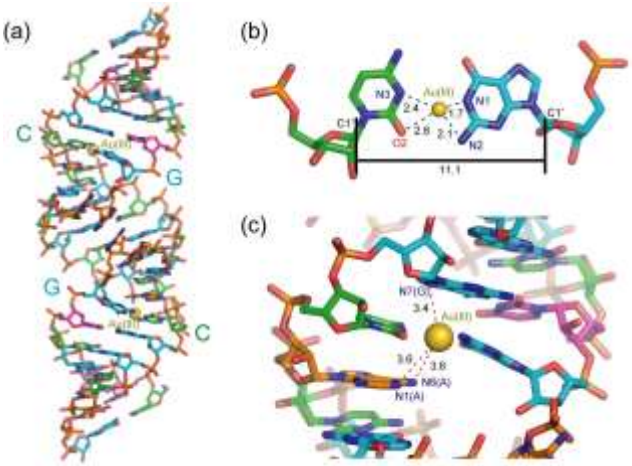

Figure 8. (a) Overall structure of the duplex form of the HIV-1 RNA dimerisation-initiation site containing C−Au^{III}−G base-pairs (PDB ID = 2OIJ).[60] (b) Detailed geometry of the C−Au^{III}−G base-pair. The C1′−C1′ distanc (Å) is represented by a solid line, and critical distances (Å) with Au^{III} are shown with dashed lines. (c) Side view of the C−Au^{III}−G base-pair. Interactions toward axial directions are represented by red dashed lines (distances in Å).

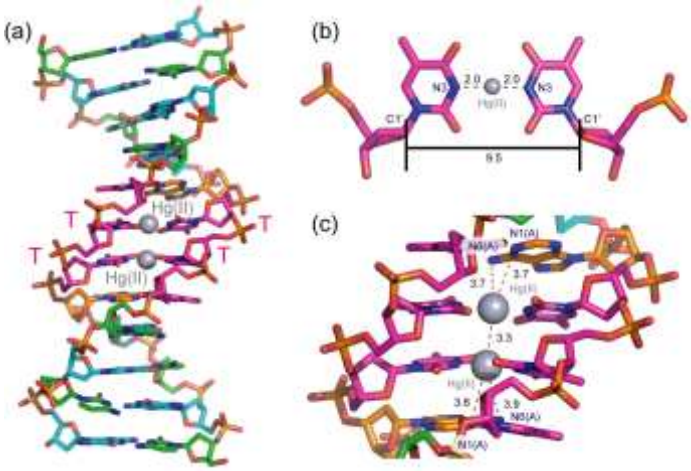

Figure 9. (a) Overall structure of the B-form DNA duplex containing two consecutive T−Hg^{II}−T base-pairs (PDB ID = 4L24).[23] (b) Detailed geometry of the T−Hg^{II}−T base-pair. The C1′−C1′ and N−Hg^{II} distances (Å) are represented by solid and black dashed lines, respectively. (c) Side view of the T−Hg^{II}−T base-pair. A possible metallophilic attraction between Hg^{II}-Hg^{II} and electrostatic interactions are represented by red dashed lines (distances in Å).

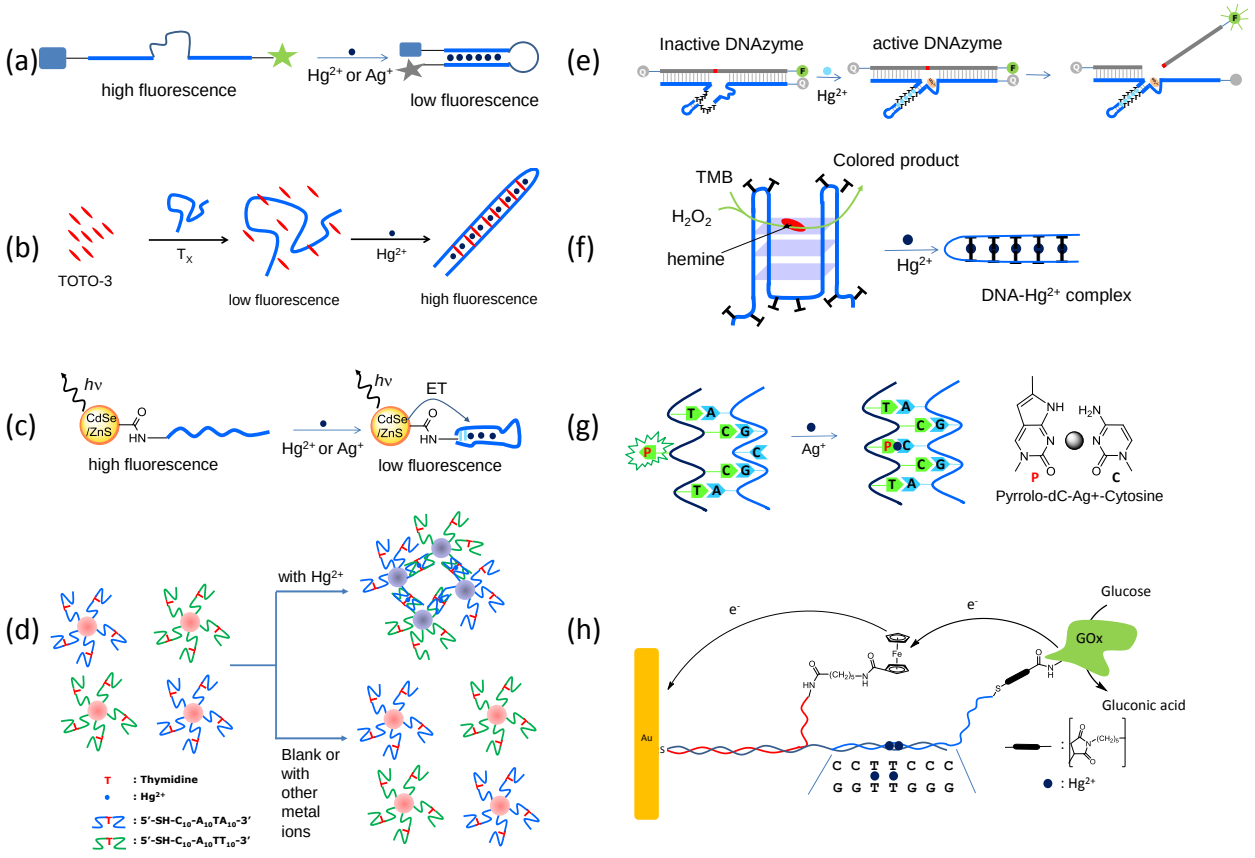

Figure 10. Sensing mechanisms for the detection of metal ions. (a) Fluorescence-off type.[5,7] (b) Fluorescence-on type.[135] (c) Quantum-dot-conjugated oligonucleotides.[136] (d) Gold-nanoparticle-conjugated oligonucleotides.[137] (e) DNAzyme.[104] (f) DNAzyme (G-quartet–hemine complex).[138] (g) Fluorescent nucleobase (pyrrolo-dC).[139] (h) Electrochemical detection.[140]

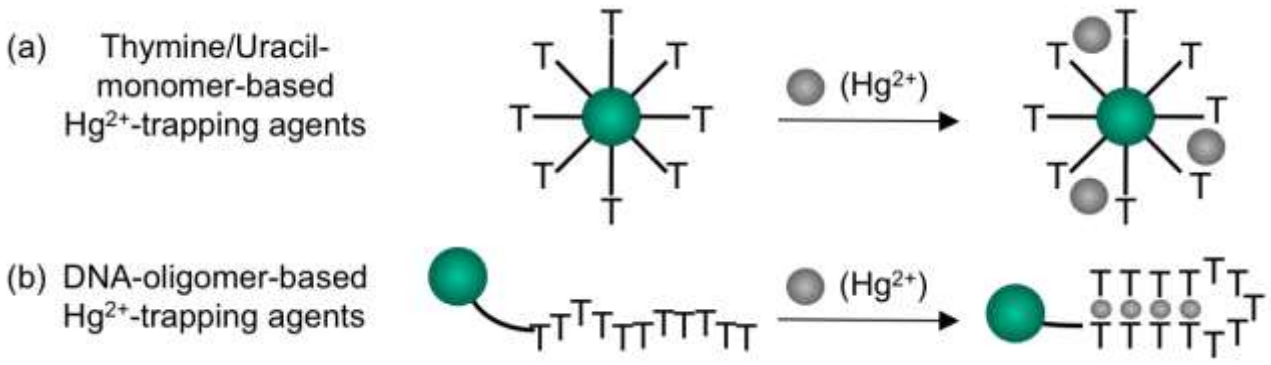

Figure 11. Two types of Hg^{2+}-trapping agents. (a) Monomer-based (thymine/uracil) agents. (b) DNA-oligomer-based agents.

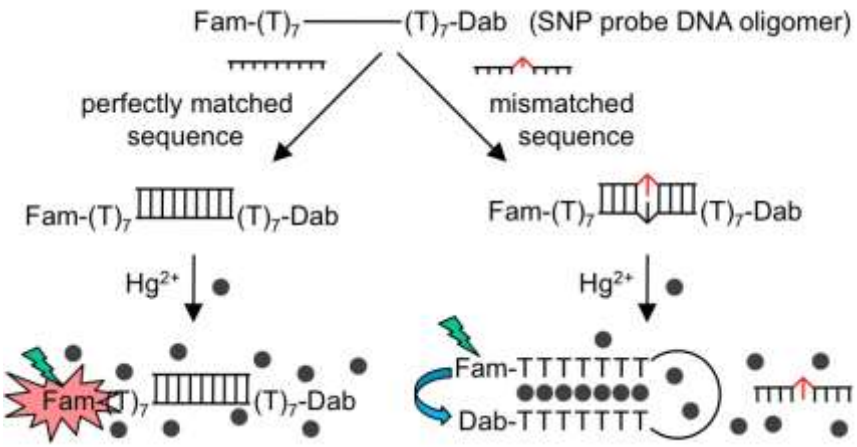

Figure 12. SNP-detection system using T–Hg^{II}–T base-pairs.

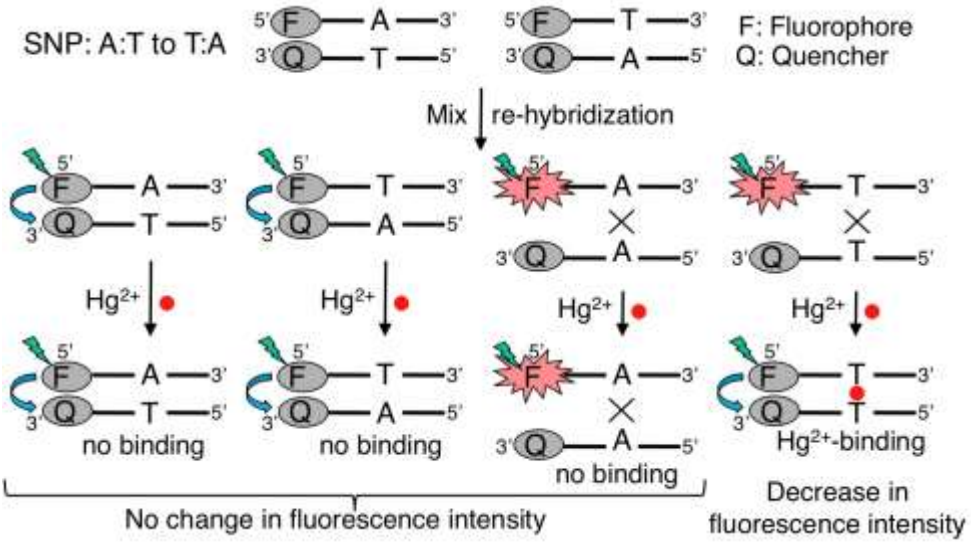

Figure 13. SNP-detection system using T–Hg^{II}–T base-pairs.

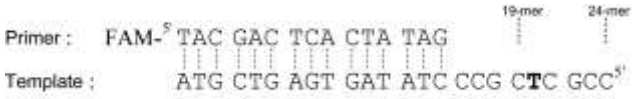

Figure 14. A template–primer complex for the formation of T–Hg^{II}–T base-pairs by DNA polymerases.

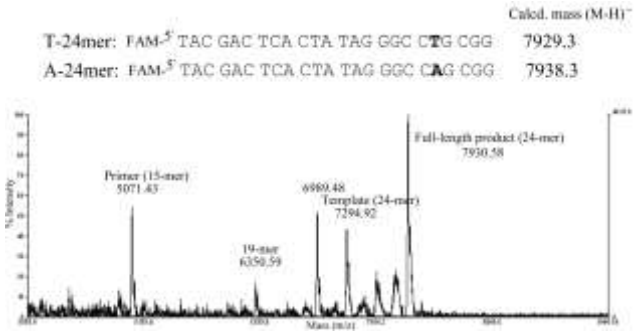

Figure 15. MALDI-TOF mass spectrum of the primer-extension product (catalysed by DNA polymerases in the presence of Hg^{2+} ions).

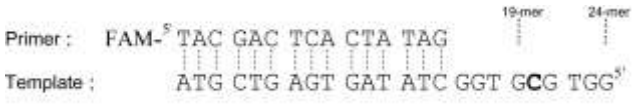

Figure 16. The template–primer complex for primer extension catalysed by DNA polymerases in the presence of Ag^{+} ions.

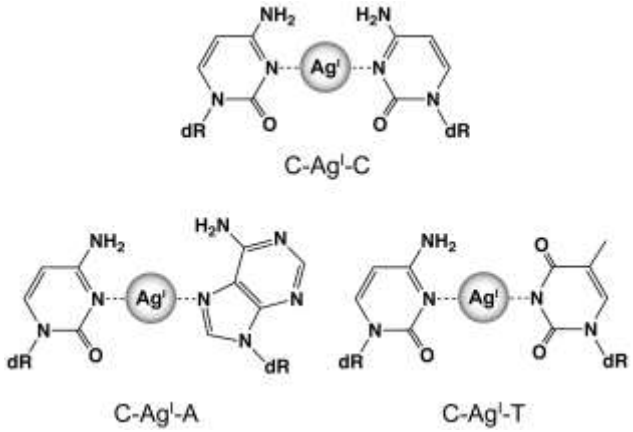

Figure 17. Ag^{I}-mediated base-pairs. The word "dR" denotes deoxyribose.

Figure 18. Regulated incorporation of two different metal ions into programmed sites by DNA polymerases.

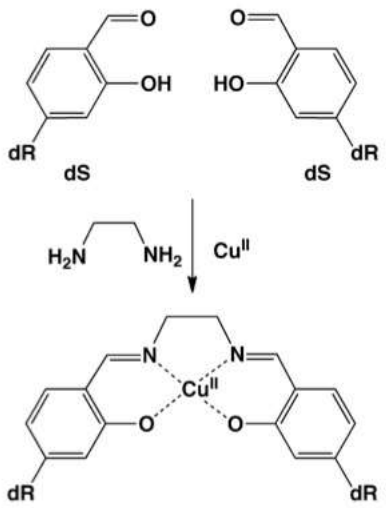

Figure 19. Formation of the S–Cu^{II}–S base-pair. The word "dR" denotes deoxyribose.

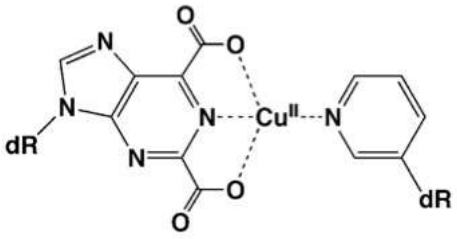

Figure 20. Pur^{DC}–Cu^{II}–3-Py base-pair. The word "dR" denotes deoxyribose.

Table 1 ^{13}C chemical shift perturbations upon binding to Hg^{2+} in the T–Hg^{II}–T base-pair[a]

Sample (M)/Solvent	Metal	Site	C2	C4	C5	5-CH_3	C6	Reference
thymidine (isolated T-Hg^{II}-T) / DMSO	Hg^{2+} (0.5 eq.)	N3	+2.7	+2.4	-0.2	+0.5	0.0	30,31
d(TT) (9.1 mM) / H_2O (pH 6.0)	Hg^{2+} (10.0 mM)	N3	+2.9[b]	+2.7[b]	N.D.	N.D.	N.D.	20
d(GCGC**T**TTTGCGC)[c] (2 mM) / H_2O (pH 6.0)	Hg^{2+} (2.0 mM)	N3	N.D.	N.D.	+0.1	+0.9	+0.4	32
d(GCGCTTT**T**GCGC)[c] (2 mM) / H_2O (pH 6.0)	Hg^{2+} (2.0 mM)	N3	N.D.	N.D.	+0.9	+1.1	+0.3	32

[a] Chemical shift changes are listed in ppm. [b] Average value of two thymine residues is presented. [c] For a DNA oligomer, the chemical shift changes of the underlined residues are indicated. Positive and negative values represent downfield and upfield shifts, respectively. N.D. = not detected.

Table 2 ^{15}N chemical shift perturbations upon binding to metal ions, and *J*-coupling with ^{15}N nuclei[a]

Sample (M)/Solvent	Metal	Site	N1	N3	NH_2	N7	N9	$^2J_{NN}$[b]	$^1J_{N\text{-}M}$[c]	ref.
T-Hg^{II}-T										
d(CGCGT**T**GTCC)•d(GGACTTCGCG)[b] (2.0 mM)/H_2O (pH 6)	Hg^{2+} (4.0 mM)	N3	–	+35.3	N.A.	N.A.	N.A.	2.4	N.D.	16
d(CGCGTTGTCC)•d(GGAC**T**TCGCG)[b] (2.0 mM)/H_2O (pH 6)	Hg^{2+} (4.0 mM)	N3	–	+29.9	N.A.	N.A.	N.A.		N.D.	16
d(CGCG**T**TGTCC)•d(GGACTTCGCG)[b] (2.0 mM)/H_2O (pH 6)	Hg^{2+} (4.0 mM)	N3	–	+30.3	N.A.	N.A.	N.A.	2.4	N.D.	16
d(CGCGTTGTCC)•d(GGACT**T**CGCG)[b] (2.0 mM)/H_2O (pH 6)	Hg^{2+} (4.0 mM)	N3	–	+30.8	N.A.	N.A.	N.A.		N.D.	16
Im-Ag^{I}-Im										
d(TTAATTT **Im** Im Im AAATTAA)$_2$ (0.5-1.4 mM)/ H_2O (pH 7.2)	Ag^+ (1.0 eq.)	N3	-3.2	-15.0	N.A.	N.A.	N.A.	N.D.	86	19
d(TTAATTT Im **Im** Im AAATTAA)$_2$ (0.5-1.4 mM)/ H_2O (pH 7.2)	Ag^+ (1.0 eq.)	N3	-3.3	-14.5	N.A.	N.A.	N.A.	N.D.	86	19
d(TTAATTT Im Im **Im** AAATTAA)$_2$ (0.5-1.4 mM)/ H_2O (pH 7.2)	Ag^+ (1.0 eq.)	N3	-5.1	-15.9	N.A.	N.A.	N.A.	N.D.	86	19
A-Hg^{II}-T										
d(CGCG**A**ATTCGCG)$_2$[b] (4.8 mM)/H_2O (pH 7)	Hg^{II} (28 mM)	N6	+15.3	-3.3	–	-0.5	-3.0	n.a.	N.D.	35
d(CGCGA**A**TTCGCG)$_2$[b] (4.8 mM)/H_2O (pH 7)	Hg^{II} (28 mM)	N6	+9.4	+2.4	–	-0.7	-1.0	n.a.	N.D.	35

[a] Chemical shift changes and *J*-coupling constants are reported in ppm and Hz, respectively. For DNA oligomers, the chemical shift changes of the underlined residues are indicated. Positive and negative values represent downfield and upfield shifts, respectively. [b] Two-bond ^{15}N-^{15}N *J*-coupling across Hg. [c] One-bond ^{15}N-Metal *J*-coupling, such as $^1J(^{15}N,^{107/109}Ag)$ derived from Ag^+ sources at natural abundance ($^{107}Ag/^{109}Ag$ = 51.8:48.2). N.A. = not applicable; – = not recorded; N.D. = not detected.

Table 3 Marker bands in Raman and IR spectra

Base-pair	Sample/Conditions	Raman / cm^{-1}	IR / cm^{-1}	Assignment	reference
T-Hg^{II}-T	d(TT)/H_2O(pH 6.5)	749	–	Marker band to probe the existence of the imino proton.	20
	d(TT)/D_2O(pH 6.5)	736	–		20
	d(TT)/H_2O(pH 12.4)	1585	–	C4=O4 stretching (major) [+ C2=O2 stretching (minor)]	20
	Hg_2•[d(TT)]$_2$/H_2O(pH 6.5)	1586	–	C4=O4 stretching (major) [+ C2=O2 stretching (minor)]	20
	Hg_2•[^{18}O4-d(TT)]$_2$/H_2O(pH 6.5)	1570	–	C4=^{18}O4 stretching (major) [+ C2=O2 stretching (minor)]	20
	Hg•(1-MeT)$_2$/crystal	1582	1583	C4=O4 stretching (major) [+C2=O2/C5=C6 stret. (minor)]	25
	Hg•(1-MeT)$_2$/crystal	537	537	in-plane ring deformation	25
	Hg•(1-MeT)$_2$/crystal	N.D.	352	in-plane N-Hg-N bending	25
U-Ag^{I}-U	Ag_3•(1-MeU)$_2$/crystal	1549	1551	C4=O4 stretching (major) [+ C2=O2 stretching (minor)]	39
	Ag_3•(1-MeU)$_2$/crystal	453	448	in-plane ring/N-Ag-N deformation	39
	Ag_3•(1-MeU)$_2$/crystal	362	362	in-plane ring/N-Ag-N deformation	39

d(TT) = thymidyl (3'-5') thymidine; 1-MeT = 1-methylthymine; 1-MeU = 1-methyluridine; N.D. = not detected; – = not recorded.

Table 4 Experimental and theoretical thermodynamic parameters

Sample (Method)	$\Delta H°$ / kcal mol^{-1}	$\Delta S°$ / cal mol^{-1} K^{-1}	$\Delta G°$ / kcal mol^{-1}	K_a / M^{-1}	n[a]	Ref.
T-Hg^{II}-T (ITC)	–3.85 ± 0.18	13.1 ± 0.65	–7.76 ± 0.19	(4.87 ± 1.35) × 10^5	1.06 ± 0.03	62
T-Hg^{II}-T (ITC)	–4.76 ± 0.13	10.6 ± 0.84	–7.91 ± 0.12	(6.34 ± 1.17) × 10^5	0.89 ± 0.02	62
T-Hg^{II}-T (Theory)[b]	–4.04	14.2	–8.27	1.16 × 10^6	1[c]	22
C-Ag^{I}-C (ITC)	–2.37 ± 0.07	18.4 ± 0.7	–7.87 ± 0.15	(5.86 ± 1.29) × 10^5	1.06 ± 0.03	63
C-Ag^{I}-C (ITC)	–2.55 ± 0.17	16.5 ± 1.5	–7.45 ± 0.29	(2.92 ± 1.13) × 10^5	1.21 ± 0.07	63
Im-Ag^{I}-Im (ITC)	–8.12 ± 1.20[d]	2.39 ± 0.48[d]	–8.84 ± 0.24[d]	(3 ± 1) × 10^6	0.9 ± 0.1	65

[a] Stoichiometry of [metal cations]/[binding site]. [b] Theoretical thermodynamic parameters of T–Hg^{II}–T base-pairs taken from reference 22 (see the references 64 for the assumed reaction pathway). $\Delta G°$ values are given for 298.15 K. The theoretical K_a was calculated from the theoretical $\Delta G°$. [c] Stoichiometry (n = 1) is an assumption. [d] Each value was converted with a conversion factor of 1 J = 0.239 cal.

Table 5 Thermodynamic parameters of tandem T–Hg^{II}–T base-pairs

		T-Hg^{II}-T	Im-Ag^{I}-Im	C-Ag^{I}-C
First	n	1.10 ± 0.04	0.98 ± 0.08	1.10 ± 0.10
	K_a / M^{-1}	(5.85 ± 2.86) × 10^5	(1.5 ± 0.3) × 10^5	(2.74 ± 1.37) × 10^5
	$\Delta G°$ / kJ mol^{-1}	-32.8 ± 1.8	-30.7 ± 0.7	-31.0 ± 1.7
	$\Delta H°$ / kJ mol^{-1}	-29.0 ± 9.1	-33 ± 0.2	-11.3 ± 8.1
	$\Delta S°$ / J mol^{-1} K^{-1}	12.9 ± 30.5	-12 ± 4	66.0 ± 21.4
Second	n	1.24 ± 0.10	1.30 ± 0.08	1.10 ± 0.10
	K_a / M^{-1}	(39.6 ± 20.1) × 10^5	(36 ± 4) × 10^5	(7.19 ± 2.51) × 10^5
	$\Delta G°$ / kJ mol^{-1}	-37.7 ± 1.8	-37.4 ± 0.3	-33.4 ± 1.1
	$\Delta H°$ / kJ mol^{-1}	-23.6 ± 5.3	-81.3 ± 0.5	-68.0 ± 7.5
	$\Delta S°$ / J mol^{-1} K^{-1}	47.2 ± 17.8	-148 ± 3	-116 ± 22
	Reference	66	65	67

Table 6 Metal arrays generated in DNA molecules

Base-pair	Number	d_{M-M}[a] / Å	Method	Ref.
S-Cu^{II}-S/T-Hg^{II}-T	10		ESI-MS, Titration(UV)	119
S-Cu^{II}-S	10		ESI-MS, Titration(UV)	120
U-Hg^{II}-U	6		NMR, Titration(UV/CD), Tm(UV)	34
H-Cu^{II}-H	5	3.7	ESI-MS, Titration(UV/CD), ESR	4
T-Hg^{II}-T	5		ESI-MS, Titration(UV/CD)	6
H-Cu^{II}-H/Py-Hg^{II}-Py	3		ESI-MS, Titration(UV)	119
Im-Ag^{I}-Im	3	3.79-4.51[b]	NMR($^{1}J_{NAg}$[c], ^{15}N-CS[d], NOE-based 3D structure)	19, 21
T-Hg^{II}-T	2	4.03-4.15	NMR($^{1}J_{NN}$[e], ^{15}N-CS[d], NOE-based 3D structure), Titration(UV/CD), Tm(UV)	16, 22, 27
T-Hg^{II}-T	2	3.3	Crystal structure	23
Dipic-Cu^{II}-Py	4		Tm(UV)	121
Dipam-Cu^{II}-Py	4		Tm(UV)	121
PyPur-Ni^{II}-PyPur	3		Tm(UV)	122

[a] Distance between metal cations. [b] The refined Ag^{I}–-Ag^{I} distance with theoretical calculations was 3.41–3.68 Å.[21] [c] $^{1}J(^{15}N,^{107/109}Ag)$. [d] ^{15}N chemical shift. [e] $^{1}J(^{15}N,^{15}N)$.